ADDIS ABABA UNIVERSITY

SCHOOL OF GRADUATE STUDIES

COLLEGE OF TECHNOLOGY AND BUILT ENVIRONMENT

CENTER FOR RENEWABLE ENERGY TECHNOLOGY

TECHNO ECONOMIC FEASIBILITY OF INSTALLING A FLOATING SOLAR PANEL SYSTEM ON HDROPOWER RESERVOIR IN ETHIOPIA

A thesis submitted to the school of graduate studies of Addis Ababa University College of Technology and Built Environment in partial fulfillment for the Degree of Masters of Science in Renewable Energy Technology

By: - Haleluya Alemayehu

ID No. GSR/4223/16

Advisor: - Solomon Tesfamariam (PhD)

June 2026

Addis Ababa, Ethiopia

CERTIFICATION

I hereby certify that I have read and recommend for the acceptance by Addis Ababa University College of Technology and Built Environment, Center for Renewable Energy Technology a thesis entitled "Techno Economic Feasibility of Installing a Floating Solar Panel System on Hydropower Reservoir in Ethiopia". This certificate is used as a partial fulfillment of the requirement for the Masters of Science in Renewable Energy Technology.

Signature -------------------

Date ------------------------

DECLARATION

I, Haleluya Alemayehu, I declare this thesis entitled "Techno Economic Feasibility of Installing a Floating Solar Panel System on Hydropower Reservoir in Ethiopia" is the result of my own work and all source or material used for this thesis have been properly acknowledged. This thesis is submitted in partial fulfillment of the requirement for Master's science in Renewable Energy Technology at Addis Ababa University and to make available at the university's Library under the role of the Library. I also declare that this thesis has not been submitted to any other institutions for the reward of any academic degree, diploma, or certificate.

Name: Haleluya Alemayehu

Signature: ____________________

Date: ____________________

Advisor Name: Solomon Tesfamariam (PhD)

Signature: ____________________

Date: ____________________

ADDIS ABABA UNIVERSITY

SCHOOL OF GRADUATE STUDIES

COLLEGE OF TECHNOLOGY AND BUILT ENVIRONMENT

CENTER FOR RENEWABLE ENERGY TECHNOLOGY

FLOATING SOLAR PV SYSTEMS INTEGRATED WITH HYDRO-POWER RESERVOIR: A CASE IN ETHIOPIA

By: Haleluya Alemayehu

Approved by the Board of Examiners:

____________________	____________________	____________________
(Advisor)	Signature	Date
____________________	____________________	____________________
(External Examiner)	Signature	Date
____________________	____________________	____________________
(Internal Examiner)	Signature	Date
____________________	____________________	____________________
(Chairman)	Signature	Date
____________________	____________________	____________________
(Director of Post Graduate Program)	Signature	Date

ACKNOWLEDGMENT

First and foremost, I would like to give Glory to God; I know no work would last without his will. I want to express my deepest, sincere gratitude to my instructor, Dr. Solomon Tesfamariam for his professional guidance and support in preparing this thesis research. I want to thank the management and employees of Ethiopian Electric Power, especially Engineer Tiruwork, the head of the generation and transmission department, who participated in this thesis by providing valuable data and information. Finally, I would like to thank my family and friends for their continuous support and encouragement during my post graduate study.

ABSTRACT

While minimizing land use, floating photovoltaic (FPV) systems are emerging as an effective method to enhance renewable energy production. This study investigate the efficiency and technical feasibility of floating solar PV system integrated with hydropower at the Grand Ethiopian Renaissance Dam (GERD) reservoir. The dam was decided as the case study region due to its enormous water surface and considered importance in Ethiopia's energy sector. In this work, a floating solar PV system with an installed capacity of 5.06 MWp was designed using PVSyst simulation software. After accounting for paths, pitch, and structural spacing, an area of 2.3% of 1 km² closed water surface area was seen as suitable for FPV installation which is 23,000 m² were utilized for the floating array. The system consists of fifteen central inverters to medium voltage transformer and the GERD high voltage substation at 220 KV. Number of modules are 11,500, 440 Wp solar panels arranged in many sub-arrays. The floating structure uses pontoon technology designed to adjust to the reservoir's water depth variations, which range from 594.16 meters to 623.38 meters, and has an anchoring cable length of 29.22 meters.

According to simulation results, the performance ratio (PR) of 80.18% with system losses of 0.17 kWh/kWp/day. The open reservoir was estimated to lose 96.587 Mm³/year to evaporation. Including floating photovoltaic (FPV) systems reduced evaporation to 89.521 Mm³/year for the small-footprint configuration and 77.270 Mm³/year for the large-footprint configuration. These reductions correspond to annual water savings of 7.066 Mm³/year (7.32%) and 19.317 Mm³/year (20.0%), respectively, demonstrating that FPV coverage can substantially mitigate reservoir evaporation losses.

Keyword: Floating solar panel, Sub array, Performance ratio, Normalized energy production, PVSyst software.

Table of Contents

LIST OF FIGURE

LIST OF TABLE

NOMENCLATURE

ABBREVIATIONS

ACXP	Annualized Capital Expenditure
A-Si	Amorphous Silicon
ATST	Advanced Industrial Science and Technology
BNI	Beam Normal Irradiance
CdTe	Cadmium Telluride
CIGS	Copper Indium Gallium Selenide
COE	Cost of Energy
CR	Captive Revenue
CRF	Capital Recovery Factor
FPV	Floating Photovoltaic System
GERD	Grand Ethiopian Renaissance Dam
GFRP	Glass Fiber Reinforced Plastic
GHG	Green House Gas
GHI	Global Horizontal Irradiance
GIS	Geographic Information System
GPV	Ground Mounted photovoltaic
GR	Grid Revenue
GWh	Giga Watt hour
HCR	High Captive Revenue
HDPE	High-Density Polyethylene
HFPV	Hybrid Floating Solar Photovoltaic
HIT	Heterojunction Intrinsic Thin layer
HOMER	Hybrid Optimization of Multiple Energy Resources

HPP	Hydro Power Plant
IREC	International Renewable Energy Congress
KW	Kilo Watt
KWh	Kilo Watt hour
LCOE	Levelized Cost of Energy
LPV	Land Based Photovoltaic
MOGA	Multi Objective Genetic Algorithm
MW	Mega Watt
MWh	Mega Watt hour
MWp	Mega Watt Peak
NASA	National Aeronautics and Space Administration
NCF	Net Cash Flow
NPC	Net Present Cost
NRB	Nile River Basin
O&M	Operation and maintenance
PID	Potential Induced Degradation
PPE	Personal Protective Equipment
PPA	Power Purchase Agreement
PSC	Partial Shadowing Condition
PSFPV	Partially Submerged Floating Photovoltaic
PV	Photovoltaic
PVGIS	Photovoltaic Geographical Information System
PVsyst	Photovoltaic System Software
RET	Renewable Energy Project Analysis Software
SP	Simple Payback Period
STC	Standard Temperature Condition

TWh	Tera Watt hour
VF	View Factor

GREEK LETTER

β	Tilt angel or slope
ɵ	Angle of incident
ρ	Albedo
γ	Coefficient of temperature (-0.0047/°C)
α	Absorptivity of the Earth's atmosphere
σ	Stefan-Boltzmann constant $W/m^2/°C^4$
Δ	Slope of the saturation vapor pressure curve (kPa/°C)
λ	Latent heat of vaporization (MJ/kg)
γ	Psychrometric coefficient (kPa/°C)

SYMBOL

G_b	Beam (direct) radiation
G_d	Diffuse radiation
G_r	Reflected radiation
G	Global radiation
GlobHor	Global horizontal irradiation
E_Array	Effective energy at the output of the array
DiffHor	Horizontal diffuse irradiation
E_Grid	Energy injected into the grid
T_Amb	Ambient Temperature
Pr	Performance Ratio
GlobInc	Global incident in cell plane

GlobEff	Effective Global, corr, for IAM and shadings
f_D	Diffuse Irradiance fraction
R_h	Ground reflected radiation on horizontal plane (W/m^2)
G_h	Global horizontal irradiation (W/m^2)
P_{DC}	Output Power of the solar panel (W)
P_{AC}	Total inverter power output
I_T	Radiation on the floating tilted surface
I_b	Beam flux
I_d	Diffused flux
r_b	Beam radiation tilt factor
r_d	Diffused radiation tilt factor
r_r	Reflected radiation tilt factor
T_w	Water temperature
T_P	FPV cell temperature (ºC)
T_w	Temperature of the water (ºC)
G	Average daily irradiance (W/m^2)
V_w	Wind velocity (m/s)
Lo	operating loss
Ep	Energy production
E_F	Open water evaporation (mm/d),
E_{FL}	FPV with large footprint
E_{Fs}	FPV with small footprint
R_n	Net radiation at the surface (MJ/m^2/d)

SW_n	Net incoming short wavelength radiation in MJ/m^2/day
LW_n	Net incoming long wavelength radiation in MJ/m^2/day
e_a	Mean daily Vapor pressure
c	Cloudiness index
$es(Tmax)$	Saturated vapor pressures at maximum temperature in °C
$es(Tmin)$	Saturated vapor pressures at minimum temperature in °C
K_d	Diffuse fraction of the global horizontal radiation
$e_s(T)$	Saturation vapor pressure at ambient temperature T in ºC
Z	Elevation (m)
RH	Mean relative humidity
f_u	Wind function in (m/s)
a_u and b_u	Wind function coefficients
D	Vapor pressure deficit (kPa)
e_a	Actual vapor pressure (KPa)
E_{PV}	Energy produced from FPV
E_H	Energy produced from hydropower
E_T	Total energy (Hydro and FPV)

SUBSCRIPT

i	Losses at the inverter
ca	Losses in AC cable
d	Daily DC energy production(day)
tr	Transmitted irradiance
m	Monthly DC energy production
r	Reference cell temperature

ce	Temperature cell
F	AC output energy of FPV
g	Energy supply to grid

CHAPTER ONE

1. INTRODUCTION

1.1. Background of the Study

For a nation to develop economically, socially, and politically energy is essential. Green energy sources are receiving more attention as the primary sources of electricity due to global warming (IREC International Renewable Energy Congress, 2015). Ethiopia is a favorable place for renewable energy growth and investment because of its vast renewable energy potential, which is spread throughout the nation. Ethiopia is known as Africa's 'water tower' because of its vast water resources and listed among the top 10 countries with the largest hydropower generation growth for 2021-2030. In addition, almost 90% of Ethiopia's green energy sources are covered by hydropower from different hydro dams and basins. The estimated available open areas suitable for hosting the FPV system from existing hydro dams and natural lakes are presented (Degefu et al, 2015).

It is one of Africa's leading renewable energy producers, with hydropower accounting for over 90% of its electricity generation. Likewise the Ethiopian Electric Power Company is attempting to add more renewable energy supplies into the electrical grid (Singh et al., 2020). Surface-mounted PVs were ineffective and needed a large amount of land because of extreme temperatures and dust. Consequently, the area required for PV installation went up for large solar farms. Floating photovoltaic systems are gaining popularity as a means of increasing PV power production efficiency as the world moves toward sustainable energy. When utilizing floating PV technology, land is no longer necessary (Gadzanku et al., 2021).

The solar panels in floating photovoltaic system are made to float on the water's surface. This technology can be placed as a hybrid floating solar plant on ponds, lakes, dam reservoirs, and other bodies of water. Furthermore, an FPV plays a major part in reducing carbon emissions and evaporating water (Gadzanku et al., 2021).

The purpose of this study is to look into how floating solar panel systems could impact Ethiopia's hydroelectric reservoirs. Ethiopia could increase electricity reliability, lower water evaporation, and diversify its renewable energy mix by combining FPV systems with its current hydropower infrastructure. It is to evaluate the technological and financial effects of installing FPV systems on Ethiopian hydropower reservoirs.

1.2. Problem Statement

Ethiopia faces significant challenges in energy access, particularly in rural areas. A floating solar panel system could help to provide renewable energy to both grid connected and off-grid communities. Our country depends on water to generate energy. Persistent droughts and irregular rainfall patterns reduce hydropower generation capacity. The mandate for electricity increased rapidly as a result of population expansion and economic development. It then needs additional resources of energy and improvement on the overall efficiency of hydropower systems.

Hydropower reservoirs lose significant amounts of water due to evaporation that contributes to water scarcity. Floating solar panel systems have the potential to address these challenges by providing a complementary renewable energy source in addition to reducing water losses from reservoir.

In order to supplement the current hydropower generation, this thesis focuses on integrating the FPV system to the Grand Ethiopian Renaissance Dam hydropower system.

1.3. Objective

1.3.1. General objective

The main objective of this thesis is technical and economic feasibility floating solar panel system that could be installed on the Grand Ethiopian Renaissance Dam (GERD).

1.3.2. Specific objective

The following particular goals will be accomplished so as to attain the main golas.

- Study the hydropower dam catchment area and surrounding,
- Determining the FPV size capacity,
- Evaluate the evaporation reduction,
- Evaluate the power and energy increase after a hybrid FPV-hydropower,
- Economic analysis,
- Comparing the findings with another research works.

1.4. Significance and Scope of the Study

This research is significant for addressing Ethiopia's energy and environmental challenges by examining the possibility of floating solar photovoltaic (FPV) systems on hydropower dams. Ethiopia's production of electricity is predominantly hydropower-based, making it vulnerable to climatic variability, including drought. This study examines how floating solar photovoltaic systems can diversify Ethiopia's energy mix by integrating solar energy with hydropower, ensuring a more reliable and sustainable energy supply.

Hydropower reservoirs in Ethiopia face significant water evaporation losses due to the country's climatic conditions. Floating solar photovoltaic systems can reduce evaporation by shading reservoirs, thereby conserving water and improving reservoir management.

Unlike ground-mounted solar systems, the suggested systems require no additional land, reducing the need to clear land or compete with agricultural or urban development. The effect on aquatic ecosystem and the complex design system is the drawback of floating PV system. In order to support Ethiopia's efforts to reduce poverty and promote economic progress, the analysis identifies prospects for increase sustainable energy generation. The technical and financial aspect of floating solar PV system are examine in this paper.

1.5. Thesis layout

This research is organized into five chapters. Chapter one: presents the introduction of the research, including background, statement of the problem, objectives, significance, and scope of the research. Chapter two: reviews the relevant literature related to the research including, an overview of floating solar photovoltaic, floating photovoltaic systems components and platform, types of solar PV module, advantage and disadvantages of FPV systems, hydropower systems and integration with floating solar system, and research gap. Chapter three: describes the research methodology, including the study of a selected area, site location for FPV installation, designing FPV structure, Solar PV design, mathematical modelling of PV system, and how the evaporation is reduced by using two different systems (large and small footprint), technical and economical feasibility and PVsyst modeling. Chapter four: presents a discussion of research result and findings with other researchers. Chapter five: provides a conclusion and recommendations for future work

CHAPTER TWO

2. LITERATURE REVIEW

2.1. An Overview of Floating Solar Photovoltaics

A lot of research has done on hybrid renewable energy system, which combines technologies to enhance energy production while reducing environmental impacts in response to the growing demand for clean and sustainable energy sources.

Solar power production technologies known as floating solar photovoltaic (FPV) systems are installed on water surfaces these systems usually take the shape of panels that are fixed a top floating platform (Qi et al., 2021). The PV module is the solar panel itself, which is the heart of the system. It captures sunlight and converts it into electricity (Shi et al., 2023). The classification of photovoltaic systems is ground-mounted, offshore, canal top, roof-mounted, and floating systems. Large land sections are necessary for ground-mounted PV systems. The power generation capacity of rooftop photovoltaic systems, on the other hand is comparatively low ranging from 5 to 20 kW for residential buildings and 100 kW for commercial buildings (Sahu et al., 2016). However, due to a lack of available land, these onshore solar technologies are unable to meet the demand for electricity. As a result, water-based PV systems including fixed and floating PV (FPV) varieties are progressively emerging as a viable option that helps meet the demand for energy. Because water cools, floating solar produces more electricity than rooftop and ground-mount solar systems (Yousuf et al., 2020). By shading the water, it also reduces the development of algae and reservoir evaporation. Very dense polyethylene, which is completely reusable and resistance to rust and ultra-violate radiation is use to make the floating structure (Sahu et al., 2016; Yousuf et al., 2020.).

Power solar inverters, PV panels, electrical cables and connections utilized underwater, the mooring system, and distinct float structures are all crucial components of FPV power systems (Koondhar et al., 2024). The floating structure is like a raft that keeps the solar panels above the water. It's made of lightweight, durable materials like buoyant materials that can float on the surface of reservoirs (Ghosh, 2023). It supports the weight of the solar panels and ensures they stay stable even when the water moves or the weather changes. The anchoring and mooring system keeps the floating solar panels in place on the water. Think of it like ropes or chains that tie the floating structure to the bottom of the reservoir or to the shore, preventing it from drifting with wind or water currents. This system ensures the panels stay in the right position to capture sunlight effectively (Qi et al., 2021). The cables and connecting wires are the "electric highways" of the system. They carry the electricity generated by the solar panels to the power grid or to storage systems. These wires are specially designed to be waterproof and durable, as they need to function in a wet environment without getting damage (Rorisang Christopher Moqulo., 2022; Qi et al., 2021).

Because of high temperature coefficient, PV systems perform worse when panel thermal stress is significant. To put it another way, the floating PV has benefits for the environmental and for conserving land and water (Lee et al., 2020). Owing to these advantages, FPV systems placed on bodies of water, including lakes, reservoirs, dams, and ponds, have already been widely implemented in various locations and expanded internationally (Farfan & Breyer, 2018). Since 2016, the installed capacity of FPV has grown dramatically due to tremendous technological advancements (Lee et al., 2020).

But putting these FPV technologies into practice necessitates carefully weighing the potential technological, financial, and environmental effects. For sustainable power generation a strong, efficient feasibility and system performance strategy is therefore required, one that can give its technological resources first priority (Alhassan et al., 2023).

2.2. Global Growth and Development of FPV System

Installing PV systems over water is known as floating PV, or flotavoltaics (FPV). Usually, photovoltaic is fixed mostly on rooftops, on the ground, or as building-integrated PV (Ghosh, 2022). But FPV is now becoming more popular. The early 2000s saw the start of FPV system development in Japan, a 20 kW FPV system was initially set up in Aichi by the Institute of Advanced Industrial Science and Technology (AIST), where the lack of available land for solar installations prompted research into floating PV as a possible remedy (Trapani & Redõn Santafé, 2015). Since then, the technology has spread throughout the world, and large-scale floating solar arrays have been established in a number of nations, including China, India, and South Korea. FPV systems have been very helpful in areas with a lot of water resources but little land.

The first people to file for inventions on floating solar were Americans, Danes, French, Italians, and Japanese. The first known invention in Italy pertaining to water-based PV modules dates from February 2008 (Trapani & Redõn Santafé, 2015). In May 2008, 994 solar PV modules total of 175 kW were installed on 130 pontoons and floated in the winery's irrigation pond at the Far Niente Winery in Oakville, California (Trapani & Redõn Santafé, 2015). Many tiny sized floatable PV fields were built within the next seven years. In July 2013, the first megawatt-size facility was operational in Okegawa, Japan (Farfan & Breyer, 2018).

In recent years, many countries have made significant efforts to advance FPV technology. Global FPV installations are widely distributed across more than 60 countries, with a capacity of 3 GW by 2021. It appears that this quick expansion will continue for some time to come (Benjamins et al., 2024). By 2030, it is anticipated that the total capacity of FPVs would reach 10-30 GW (Shi et al., 2023).

In addition to the technological advancements, the harmful emission from sources of fossil fuel have decreased globally as a result of worldwide investment in revolutionary low-carbon energy solution, like strategic sustainability efforts, like renewable energy (RE) (Gunfaus & Waisman, 2021).

2.2.1. Floating photovoltaic structure components

Freshwater bodies are currently the focus of floating solar photovoltaic applications. Nonetheless, there is still a huge amount of renewable energy available, since seas occupy approximately 70% of the planet's surface. Therefore, it is natural to move floating solar applications from offshore to nearshore locations. Because of the difficult marine settings and the consequent need for the floater to withstand high wave stresses, it is expected that these applications would become increasingly complex (Cazzaniga et al., 2018a). FPV on seawater has two challenges, environmental pressures (mostly wind and wave impact) and salt corrosion. The floater's materials must be appropriate for the water environment, with durability being a crucial factor that subsequently affects cost. For instance, the material must be impervious to corrosion from sea water and able to tolerate stress breaking from wave loads (Niccolai et al., 2024).

Pontoons or separate floats, mooring systems, PV modules, underwater cables, electrical connections, and inverters are the primary part of an FPV system, according to numerous researchers (Koondhar et al., 2024). Indicating the connections between PV modules is one of the most crucial parts of designing PV systems, especially when partial shadowing condition (PSC) is present (Exley et al., 2021).

Pontoons

One kind of flotation device with enough buoyance to float both by itself and with a heavy load is a pontoon. Depending on the needs and available space, in a series-parallel architecture, the platform may accommodate an appropriate number of modules (Ghosh, 2023). In Spain (Agosto Alicante), a 350 m^2 FPVS model with a 20kW output power was constructed using reservoirs and was the subject of both scientific and economic evaluation. Following the prototpe's successful operation, 1458 PV panels covering 4490 m^2 were installed on a large scale using 750 pontoons (Abid et al., 2019; Koondhar et al., 2024).

The tilt of the pontoon is affected by the wave's passage. When the pontoon is first bent, the angle of reflection between the solar beam and the module's standard is θ_0. As shown in Figure 2.1, the pontoon then tilts during the wave passage, changing the angle of incidence to $\theta_0 + \theta$waves (Tina et al., 2021).

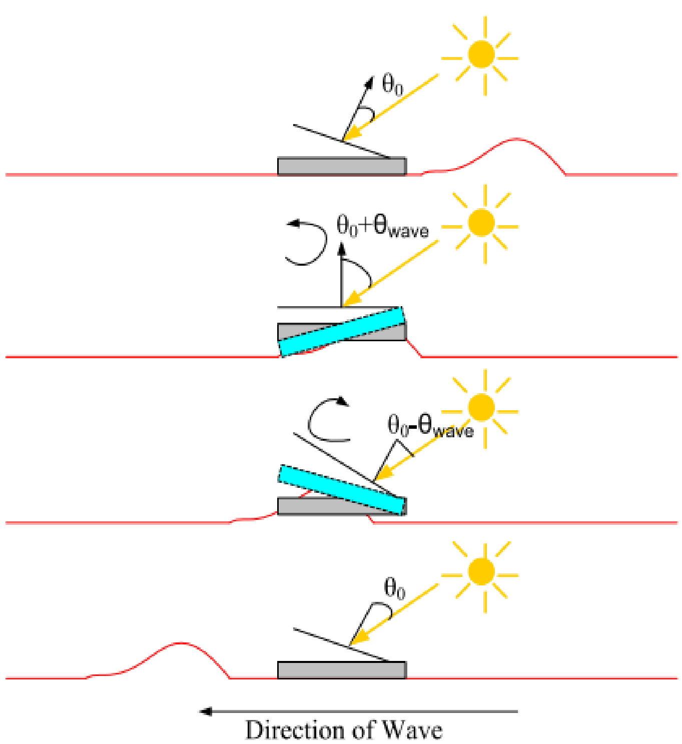

Figure 2. 1 A) Influence of the waves on the pontoon B) Structure of pontoon (Tina et al., 2021)

Single PV modules may experience slight tilt varation because waves impact the placement of the entire PV system in the case of rigid floating devices and no-rigid floating systems. The type of floated structure influences how tilt fluctuation alters it (Koondhar et al., 2024). In this case, an imbalance in irradiance between modules that belong to the same string might be used to calculate losses. The fact that floating PV systems are usually designed for usage in water basins with suitable conditions (low wind and waves) must be emphasized (Gorjian et al., 2021).

High-density polyethylene (HDPE)

High-density polyethylene (HDPE), which is well-known for its accuracy, conventional durability, UV resistance, and corrosion resistance is typically used to make floating devices (Yousuf et al., 2020). Platforms for floating objects can be made from Glass fiber reinforced plastic (GFRP). To create a larger float, raise the quantity polyethylene pores that are weight-effective. The majority of direct water contact really happens through completely HDPE rafts or HDPE pipes supported by galvanized steel frames (Solomin et al., 2021). Another way to save water is to cut evaporation by as much as 70%. Furthermore, a 6% increase in power gain is brought about by the PV's downstream cooling. The cooling effect of water generates more electricity than floating solar supports and rooftops (Perera, 2020). Figure 2.2 is chosen for its durability, corrosion resistance, and ability to stay afloat despite bearing the weight of solar panels and other components.

Figure 2. 2 High-density polyethylene (HDPE) material (Perera, 2020)

Mooring System

The floating PV systems are kept in place and prevented from floating away or turning down by a mooring system, which consists of any quays, wharfs, jetties, piers, anchor buoys, and mooring buoys. For deep water, these devices are costly (Ghosh, 2023). The PV system is secured and keep the floating system steady. As Figure 2.3 mooring system, which consists of connectors, an anchor, and mooring string, can be used to connect a floating platform at any depth of water. An anchor on the ocean floor is connected to a floating object by a mooring line (Do Sacramento et al., 2015).

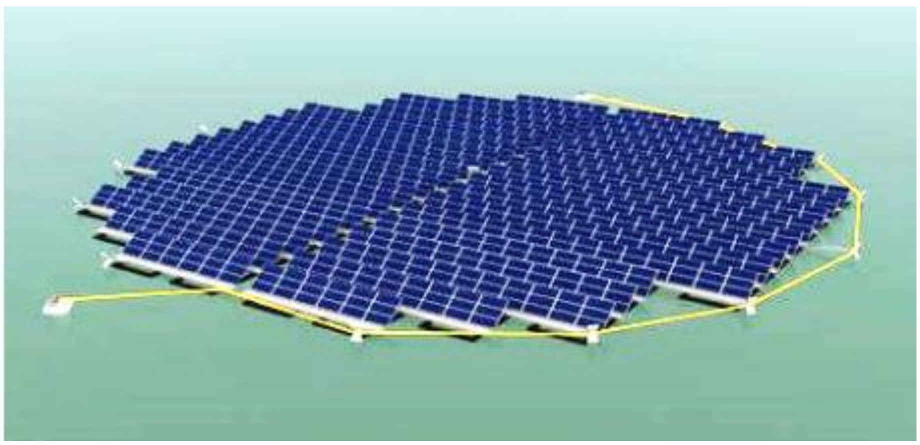

Figure 2. 3 Mooring system of floating PV with active cooling design (Ghosh, 2023)

2.2.2. Solar PV module

Floating solar systems have up till now utilized conventional crystalline silicon solar modules. Furthermore, specially made modules must be exposed to salty, moist conditions for an extended period of time as more and more designs are placed on the saltwater surface. Since practically all metals corrode over time, polymer frames and other supports are needed to replace conventional aluminum frames (Yousuf et al., 2020). As a result, instead of using typical metal frames, a different material will have to be employed. In fact, second-generation solar panel technologies including copper indium gallium selenide (CIGS), amorphous silicon (A-Si), and cadmium telluride (CdTe) are viable options for floating PV systems (Luo et al., 2021). Due to their relative infancy in terms of development and deployment, third generation PV technologies are not currently utilized for FPV systems (Jiang et al., 2023).

Figure 2.4 PV modules for FPV systems is crucial since they must survive extreme climatic conditions like as humidity, water exposure, and mechanical stress. Choosing good solar panel for a floating solar panel system depends on efficiency, durability, cost, and environmental condition.

Figure 2. 4 Floating solar photovoltaic system (Jiang et al., 2023)

A. Thin-film solar panel

Thin-film modules are made from layers of photovoltaic materials like amorphous silicon, cadmium telluride (CdTe), or copper indium gallium selenide (CIGS). This module, noted for their flexibility and lightweight design, are becoming a popular choice for floating solar systems (Subodh Mahajan., 2023.). Their reduced weight per square meter makes them excellent for floating constructions, although they are often less efficient than crystalline panels. However, lower efficiency 17-19% and shorter lifespan limit their performance.

B. Second generation CdTe solar panel

In CdTe solar panels, the light-absorbing layer is a thin layer of cadmium telluride. Because of their cheap manufacturing costs and excellent conversion efficiency, CdTes are widely used for large-scale installations. In addition, compared to some other technologies, CdTe panels are less vulnerable to extremes of heat and light (Velu Kaliyannan et al., 2021).

C. Amorphous Silicon (A-si)

The silicon used to make non-crystalline A-Si solar cells allows for flexibility and lightweight design. Even though A-Si panels have weaker efficiency of conversion compared to other systems, they work better in situations with scatter lighting, including days with clouds or places with less light. Because of this feature, they can be useful for floating photovoltaic applications where conditions of light can change due to surface ripples and reflections (Mayville et al., 2020).

D. Copper Indium Gallium Selenide

Copper Indium Gallium Selenide (CIGS) solar panels are made of thin copper, selenide sheets, gallium, and indium because they have high conversion efficiencies and perform well in low light conditions. CIGS panels are renowned for their adaptability to uneven or curved surfaces. The flexibility can be useful for floating solar panels installation that would need to be adjusted to fit the arc of the water body (Wijewardane & Kazmerski, 2023).

E. Monocrystalline solar panel

Monocrystalline solar panels are the most efficient type of solar panel currently on the market. It made from single crystal silicon offering 18-22% efficiency (josh jackman, 2024). Monocrystalline panels are a common option for floating solar plants due to their excellent efficiency and durability. Their capacity to function well in low-light circumstances makes them ideal for environments where sunlight may be partially obscured (Ma et al., 2024).

F. Polycrystalline solar panel

Polycrystalline modules are constructed of multiple silicon crystals, resulting in a somewhat lower efficiency 15-17% but a reduced cost (josh jackman, 2024). Lower efficiency requires more panels to provide the same quantity of power. In humid and rainy environments, polycrystalline panels are less durable than monocrystalline panels (Subodh Mahajan., 2023).

G. Mono-facial solar panel

Mono-facial solar panels are the oldest and most widely used type of solar panel. They only generate power on the front side of the panel, where sunlight directly contacts the photovoltaic (PV) cells (Tina et al., 2021). For decades, these panels have been the solar industry standard, and they are widely used in rooftop and ground-mounted solar installations, as well as certain floating solar PV (FPV) systems.

H. Bifacial solar panel

Bifacial panels generate power from both the front and back sides. The rear side collects reflected light from the water surface, increasing energy output by 10-20% compared to mono-facial panels. Additionally, it reduces the cell's working temperature and increases maximum power production by reducing infrared absorption (Guerrero-Lemus et al., 2016). Studies on bifacial PV modules show a 50% increase in energy yield compared to standard solar PV kinds (Gu et al., 2020a).

Due to its low manufacturing expenses, stable efficiency, and natural available, silicon is the preferred natural source. Generally, 4-17% of solar radiation is converted into electrical energy b PV. As shown in Table 2.1 below the present solar panel technology's negative coefficient of temperature and mean efficiency are listed. (Nguyen et al., 2023).

Table 2. 1 Efficiency characteristics of photovoltaic cell (Nguyen et al., 2023)

Photovoltaic cell technologies	Temperature coefficient (% / °c)	Efficiency (%)
Monocrystalline Silicon	-0.45	16-21
Polycrystalline Silicon	-0.45	13-17
Heterojunction with intrinsic thin layer (HIT)	-0.29	18-20
Amorphous Silicon	-0.21	6-9
Cadmium telluride (CdTe)	-0.25	8-16
Copper Indium Gallium Selenide (CIGS)	-0.35	8-14

Under water Cables and connectors

Power is produced and distributed to the nearby location by the solar system. Consequently, electricity can be stored in batteries or sent into the grid. Instead of being pulled underwater, the wire in the approved project has stayed on the water's surface. Solar floating systems require waterproof junction boxes with an IP67 rating, but no submerged electrical lines or components (Yousuf et al., 2020.). Additional electrical equipment, such as solar PV inverters and batteries, remain dry at the installation site. In Figure 2.5 power cables are designed to be waterproof and resistant to extreme temperatures, potentially extending system life.

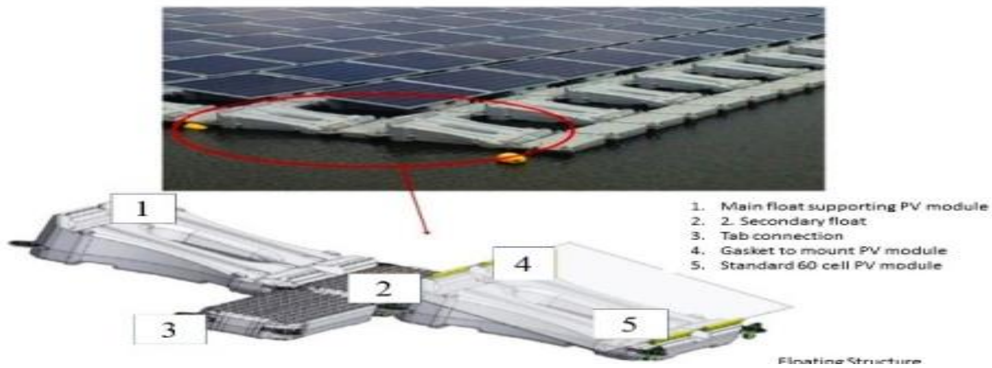

Figure 2. 5 Under water electrical cables and components (Sahu et al., 2016)

2.2.3. Advantage and impact of FPV system

2.2.3.1. Advantage of FPV system

The main causes of the increase and rapid growth of floating solar are the high demands on rooftop space and land resources, clashes with other sectors of the economy, such as tourism or agriculture, as well as the reduction in efficiency at high cell temperatures. Sometimes the ground-mounted systems are situated in isolated areas, necessitating expensive infrastructure (like a substation), and other times the project is situated in challenging regions, like mountainous or unstable terrain, requiring additional site preparations (earthworks) (Oliveira-Pinto & Stokkermans, 2020). Floating photovoltaics offer a fantastic solution to eliminate land consumption, but their cost is similar to that of plants found on land-based. Numerous writers have emphasized the technology's many benefits in the literature. The list needs of FPV are:

- Floating solar systems make use of underutilized water bodies, such as lakes, dams, and resirviors, eliminate the need to clear natural landscapes for solar farms or repurpose fertile agricultural land (Cazzaniga et al., 2018b).
- It saves money by doing away with the requirement to rent and prepare land for installation. additionally, integration and transmission infrastructure costs may be reduced due to the close proximity to the electrical infrastructure already in place at neighboring hydroelectric plants or water treatment facilities (Oliveira-Pinto & Stokkermans, 2020)
- The shading effect is minimum since it is situated in open area
- A decrease in growth of algae and the shading effect of solar arrays can significantly reduce water evaporation (Amer et al., 2023).

- FPV systems, are an effective way to take advantage of the cooling effect by placing PV modules on bodies of water. The modules' efficiency is increased by this cooling action, raising the yearly energy output. According to studies, depending on the local climate, when in comparison to GPV systems, this effect of cooling can result in an efficiency boost for FPV systems of a rate of 1.5 to 12.5% (Micheli, 2022).
- The albedo effect, which increases the effectiveness of floating solar panels, is facilitated by the natural reflective qualities of water bodies. The quantity of photons that can be transformed into energy is increased when sunlight is reflected off the water's surface and back onto the solar panels. Because of this mutual relationship, which increases the total energy yield, floating solar systems are a desirable option for maximizing solar energy production (Rosa-Clot et al., 2017).
- Floating solar system use current available module and cleaning is easy,
- FPV with hydroelectric plant mainly support day-time peak load for evening peak. Dry seasons corresponding to high solar irradiation months, this reduces seasonal variability (Liu et al., 2018).
- Reduction of power fluctuation occurs due to floating PV panels give the maximum energy production during hot (dry) season while the hydroelectric power plant registers a reduction of power due to seasonal water cycle (Cazzaniga et al., 2019).
- Installation and decommissioning of FPV is simple and straightforward. The most significant distinction is that, unlike the foundations used for a land-based plant which are much more permanent and intrusive, floating systems have no fixed structures and the mooring of systems can be installed and removed in a totally reversible way (Cazzaniga et al., 2019).

2.2.3.2. The draw backs of FPV system

Some researchers have identified the advantages of floating solar photovoltaic systems over ground photovoltaic systems, as well as their consequences and draw back. They are:

- Humidity can impact FPV placement near water. GPV is more affected by humidity compare to FPV, since FPV module can endure increase humidity. High humidity in the surrounding might significantly affect module performance (Kaplanis et al., 2023). By increasing the cell temperature, which can lower the output voltage and current, high humidity levels can reduce the efficiency of PV panels.

- In pilot projects, floating solar has proven to operate dependably for over a decade. Their long-term durability is still up for argument, though. More information is required to understand how these systems endure decades of exposure, taking into account elements like weather-induced wear, performance deterioration over time, and the effects of continuous maintenance throughout the course of their operating life (MIBET ENERGY 2024,.).
- Wind and wave loads are applied to the modules, which could result in microcracking, which would reduce output and cause durability problems (Sahu et al., 2016).
- Ground-mounted PV installations are intended to operate for 30 to 40 years, whereas floaters are usually built for a 25-year lifespan. The installation of these systems may have an impact on transportation activities like fishing (Sahu et al., 2016).
- Corrosion of floating structures, primarily from float degradation from UV exposure. Extreme wind loads, water depths, water level fluctuations, and waves must all be taken into consideration while designing station-keeping (Liu et al., 2018).

2.3. Floating Photovoltaic System Platform

For FPV structures, there are many different kinds of floatable platforms that may be approximately divided into:

Buoyance-based platforms

The most widely used FPV platform is made up of multiple buoyant components joined together to create a stable floating foundation. These stages are frequently inexpensive, modular, and easy to assemble and disassemble. However, they are less stable in turbulent water and may flood more often due to their low freeboard height (Solomin et al., 2021).

Tension leg platforms

As seen in Figure 2.6, tension leg platforms permit wider FPV systems and are more stable, but they are extra costly and difficult to install and maintain than other platform type due to their use of tensioned cables to anchor to the seafloor (Conference Services Ltd, 2022).

Semi-submersible platform

As shown in Figure 2.7 by partially submerging in water, a semi-submersible platform can improve stability and reduce the likelihood of flooding. However, it is expensive because of having more intricate installation and maintenance requirement when compared to buoyancy-based platforms (Li et al., 2022). It might be a way to clean panels, lower reflection losses, and increase efficiency by getting rid of thermal drift. This submersible photovoltaic system works well in low-latitude areas when both irradiance level and ambient temperature are quite high throughout the year (Solomin et al., 2021).

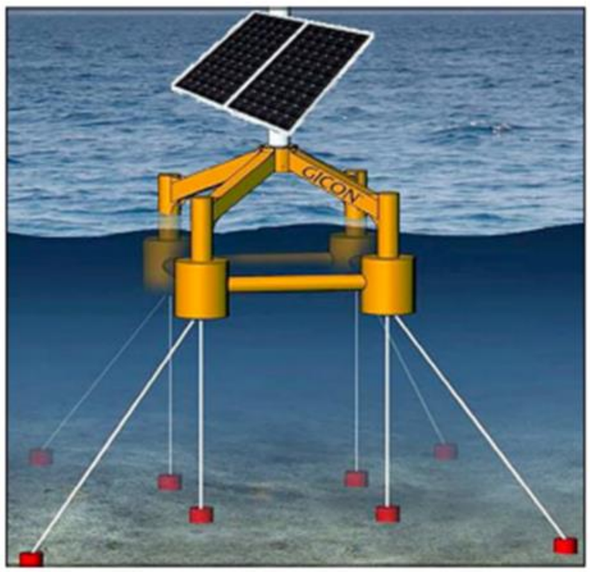

Figure 2. 6 View of tension leg platform (Solomin et al., 2021)

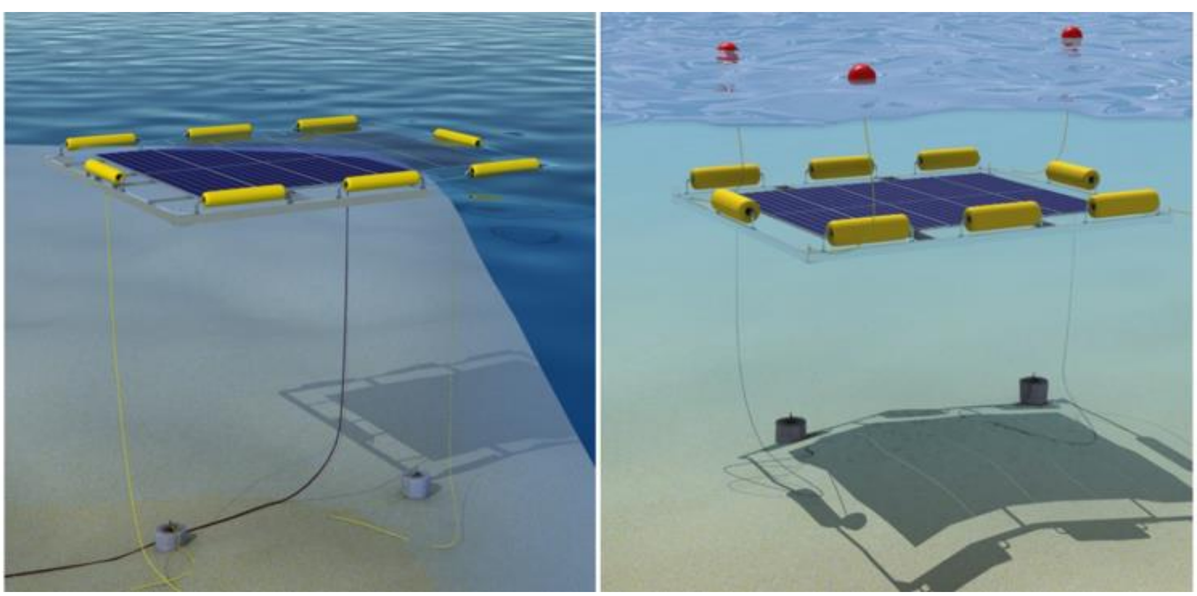

Figure 2. 7 Design of semi-submersible/fully-submersible platforms (Solomin et al., 2021)

Floating rafts

As seen in Figure 2.8, solar power plants are installed on several pontoons that are anchored to the bottom of the ocean to create floating rafts. These standard rafts are simple to erect and maintain, but because wave conditions might compromise their stability, they may be more likely to capsize in turbulent waters (Refaai, M.R.A. et al. 2022, n.d.).

Figure 2. 8 Solar powered floating rafts (Cazzaniga et al., 2018b)

2.4. Installation and location criteria

Building FPV systems the anchoring and mooring mechanism is not complicated. FPV systems are often built on land before being transferred to the water, where they may be readily transported to the planned installation site without the need for sophisticated machinery. When deciding where to put FPV, a number of variables must be taken into account. The main criteria that need to be considered when choosing a site for FPV are listed in below. An FPV system may be impacted by a number of factors, including weather, location, topography, and water quality (Amer et al., 2023). The system's location is crucial since the site's latitude and longitude influence how much solar energy it receives. The areas close to the equator receive more solar energy than the areas near the poles. Ground and sea factors can affect how well the anchoring system provides stability and safety in hazardous maritime settings. The floating when selecting a location for FPV installation, a number of variables must be taken into account (Amer et al., 2023).

- Water condition: fresh water with minimal saltwater, hardness, and wave activity

- Ground condition: typical compact soil that is appropriate for anchoring (Quek et al., 2018)
- Location: Lack of shadowing from nearby structures or mountains; proximity to an electrical outlet; and ease of installation and maintenance.
- Weather: Abundant sunlight, low frequency of fog or rain, and a wind speed of not much more than 30 m/s (Quek et al., 2018).

2.4.1. Electrical safety on FPV installation

Electrical safety standards are necessary to create FPV systems that are dependable, secure, and safe. This is primarily because proper grounding, insulation, and training can prevent corrosion and electric shock. By installing safety devices like circuit breakers and surge protectors, FPV's electrical system is protected from hazards and overloads (Amer et al., 2023). Lockdown/tag-out procedures, sufficient training, and personal protective equipment (PPE) ensure worker safety. The integrity of the system is also guaranteed by routine maintenance, which includes corrosion testing and component replacement (Kumar et al., 2021). Electrical safety consideration, including component placement, cable management and grounding requirement, should be made throughout the design phase. When all applicable rules and regulations are followed, FPV system can function safely and effectively.

2.5. Solar Radiation Components

Fortunately, solar rays travel through the atmosphere and clouds before reaching the earth. As atmospheric conditions change over time, so do the atmosphere's effects on radiation absorption and scattering. It distinguishes between beam (or direct) radiation (G_b), which passes straight through the atmosphere to the ground, and diffuse radiation (G_d), which has been spread through the air and clouds (MARCO ROSA-CLOT, 2018).

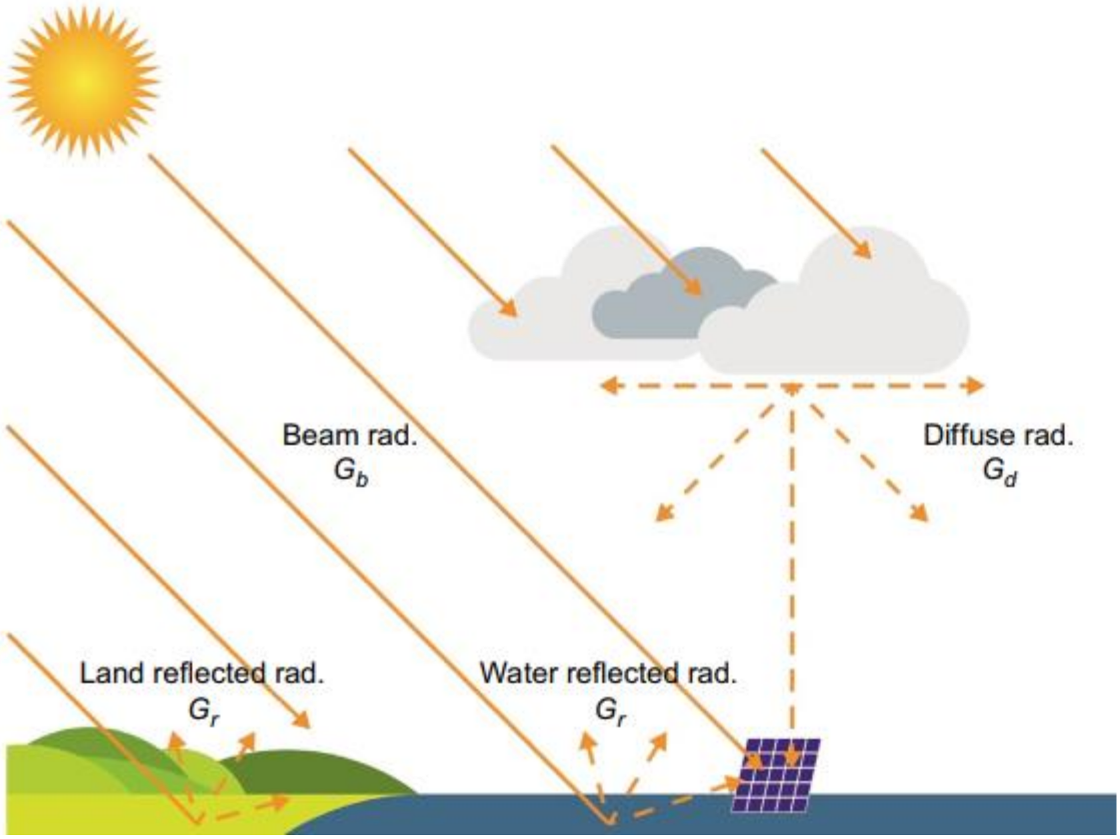

Figure 2. 9 Parts of solar radiation that hit the FPV module and the ground (MARCO ROSA-CLOT, 2018)

In Figure 2.10 it is important to note that another factor needs to be taken into account: reflected element Gr, which is bounce off the ground or the water. The total of G_b,G_d and G_r is the global radiation that reaches the FPV module. The angle of incidence (ɵ) between the line drawn perpendicular to the PV surface and the received beam radiation determines Gpv,b insolation reaches an arbitrarily aligned PV surface. Gpv,d diffuse radiation on a collector is much more difficult to estimate accurately, however it is depended on tilt angle (β). The final component of insolation striking is caused by radiation reflected by surfaces in front of a solar module. The simplest model depends on the material's reflection properties, assumes a large horizontal area in front of the collector, and has a reflectance of albedo (ρ).

2.6.1. The Albedo

Albedo is the percentage (or relative value) of solar radiation that a surface reflects in compared to the total amount of incident light. The water albedo model is a measured combination of three factors: sun shine, whitecaps, and water-leaving reflectance. There has been comparison with other models (Feng et al., 2016).

The ratio between the ground-reflected radiation to the global horizontal irradiations in equation 2.5 is albedo as indicated in (Ineichen et al., 1990) paper.

$$\rho = \frac{R_h}{G_h} \qquad 2.1$$

Where ρ is albedo, R_h is ground reflected radiation on a reverse horizontal plane (W/m^2) and G_h is global horizontal irradiation (W/m^2). Ineichen notes that albedo for water surface is typically less than 5% for most solar zenith angles, which is much lower than land surface.

Albedo on water has a complex dependence on wind intensity, light wavelength, and water surface characteristics (waves and sun glint), but it is always fairly limited and is usually less than 5% for interesting azimuth angles ($\gamma s > 60$), according to all of these detailed analyses. In comparison, the albedo effect on land can vary from 20% for grass or sand surfaces to at least 60% when ice or glaciers are available (MARCO ROSA-CLOT, 2018).

2.7. Hydropower System and Integration with Floating Solar System

2.7.1. Overview of hydropower system

Many regions of the world today use hydropower renewable energy source to go along with their electrical demand. Primarily in 250 BC stated that the usage of hydropower was to power the clock by water. From that time, hydropower has developed from powering a little clock to producing enough power huge town. Water wheels were used in early innovations to power water pumps and mill stones, followed by industrial machinery. For many ages, water has been used as the source of energy (Bernt Lamark et al., 1998). Usually hydropower production capacity mainly focused on massive high head power plants that giving their output to the national electricity grid.

Currently under construction, the Grand Ethiopian Renaissance Dam (GERD), formerly known as the Millennium Dam and occasionally called the Hidase Dam, is a gravity dam on Ethiopia's Blue Nile River. It is located in Ethiopia's Benishangul-Gumuz Region, some 40 kilometers east of the Sudanese border (Samaan, 2019). The Ethiopian government claims that the dam is 90% finished as of April 2023. When ended the 6,000 MW dam will rank eighth globally and be the biggest hydroelectric power infrastructure in Africa. With a capacity of 72 billion cubic meters and an area of 1,874 km^2, the reservoir would rank among the biggest on the continent (Samaan, 2019).

2.7.2. Hybrid FPV with hydroelectric power plants

Researchers are looking into combining FPV systems with hydropower plants to boost the potential of hydropower. Floating PV modules are connected to hydropower facilities that are already in operation to build hybrid systems. The combination of FPV with hydropower has several advantages. It can improve water quality, increase the efficiency of hydropower, and reduce water evaporation which increase the availability of water and reduced head losses by limiting algae development. Because FPV systems could possibly be installed in locations with existing grid connections, installation costs are reduced. The inconsistency of solar energy may be managed by combining FPV and hydropower if the reservoir can hold water even when the FPV system is not producing electricity. Research indicates that FPV-HPP hybrid systems can improve co-production of food, energy, and water.

2.7.3. Recent research findings

Big dam (EliGetieas Mandefro & Jember, 2022), wrote a paper on Renaissance Dam in Grand Ethiopia might be utilized for a system of floating solar to get rid the requirement for transmission infrastructure and land. Given the reservoir's bigger area of around 1,874,000,000 m^2, the Renaissance dam's potential for solar PV floating installation needs to be investigated in order to meet the electricity demand in Ethiopia's business, industrial, and residential areas. Additionally, the water's cooling effect on the PV floating keeps it efficient and boosts the panels' power output. The PVsyst software package is used to model and simulate the proposed FPV plant.

Lastly, the analysis shows that the GERD can produce a maximum power of 18,740 MW. Its effectiveness was assessed using a 1 MW connected to the grid FPV system. The use of FPV in conservation of water, reduction of CO_2 emission, and production of energy is stated (EliGetieas Mandefro & Jember, 2022). The conserved water of GERD yearly by the construction of 1 MW FPV was 54.4 million liters, which helps the downstream nations of the Blue Nile preserve their portion of water.

In order to evaluate its extent and compare it with an on-ground solar system with comparable specifications, Hafeez et al (Hafeez et al., 2022) attempts to estimate the possible installation of a floating photovoltaic system on an urban lake location. The one-year capacity factor under standard temperature settings (STC) is 0.70% greater when a 10 °C temperature drop is considered. This leads to an additional energy yield of 64 kWh/kW and 4.47 MW power potential for NUST Lake. Every 1 MW FPV system would have 11.6% yearly water reduction (Hafeez et al., 2022). The on-ground system's net present value drops under normal temperature circumstances, whereas the floating photovoltaic system's net present value stays positive because there is no land costs involved.

The Nasir et al (Nasir et al., 2023) proposed a hybrid system that includes 200 MW of Paras pumped storage hydropower, 30 MWp floating solar PV and 300 MW of conventional Balakot hydropower to examine an economical and sustainable strategy for improving the nexus of food, energy, water, and ecosystems in arid areas. This analysis uses floating solar PV systems, water stream considerations, and traditional hydropower resources to determine the leveling cost of energy storage. The hybrid arrangement may provide an additional 3693 GWh of clean energy when compared to green field continuous pumped storage hydropower, which will increase revenue by 30% over a 30-year period (Nasir et al., 2023).

The findings (Exley et al., 2022) demonstrated that FPV coverage had a substantial impact on temperature characteristics, leading to very varied effects on phytoplankton species composition and biomass. Both surface coverage and array site location often had an impact on phytoplankton. A decrease in phytoplankton biomass as a result of higher FPV coverage offset changes in the species composition of phytoplankton. By placing the FPV array on the faster-flowing portion of the water body rather than the central or slower-flowing sections, we found that the same reductions in phytoplankton biomass could be achieved with less FPV coverage.

Sutanto et al suggest installing a thermosiphon for a passive cooling to improve the performance of floating PV (Sutanto et al., 2022). According to experimental research floating photovoltaic generate about 4.52% more electricity and use of thermosiphon cooling PV increases 7.86% output power when compared to ground PV generation (Sutanto et al., 2022).

The effectiveness of partially submerged floating photovoltaic system (PSFPV) examines by Elminshawy et al as unique methods for gathering energy of solar and producing electricity on calm water surfaces in Egypt’s hot climate (Elminshawy et al., 2022). The PSFPV system is passively cooled helps to have lower operational temperature about 15.10% and produces up to 20.76% more electricity compared to the ground-mounted photovoltaic (GPV) system since, the submerged portion is in direct contact with the surrounding water. The PSFPV system exhibits a drop in LCOE from 0.075 to 0.067 ($/kWh) when the submerged length is increased from 4 to 24 cm (Elminshawy et al., 2022).

Brazil depends on hydroelectric plants, although hydrogenation has been negatively impacted by increasingly frequent droughts (Moraes et al., 2022). Brazil's electricity demand might be sustainably met by putting in place floating photovoltaic (FPV) systems in hydropower reservoirs that already exist, which would reduce evaporation losses and during dry seasons, provide more electricity to help offset hydroelectric production (Moraes et al., 2022).

Table 2. 2 Recent review paper summery

Author(s)	Specific of the research	Technical type/method
(Alhassan et al., 2023)	The FPV-Hydro hybrid plant was suggested and examined in this study. The Akosombo Dam reservoir of 420 MWp FPV, which produces 4.66 kWh/m^2/day of solar energy, was examined from a techno-economic and environmental standpoint. It worked and saved 73,327 m^3 of water from evaporating, adding an additional 10 MWp of hydroelectric power.	- RET Screen Expert software - Modelling solar PV output power performance and evaporation reduction calculation - Economic performance and environmental impact modelling
(Irshad et al., 2024)	Study demonstrate that one of the most dependable and cost-effective alternatives is to use hybrid pumped hydro storage and floating photovoltaic. By increasing net present cost (NPC) it reduces the energy cost (COE). The current FPV system reduce the evaporation fraction by 17,279,400 cubic meter and covers 4.65 km^2.	- To model the system Multi objective genetic algorithm (MOGA) is utilized. - Numerical algorisms
(Cazzaniga et al., 2019)	An overview of the advantages of PV-Hydro coupling was provided by the integration of PV	- NASA and PVGIS help to collect data

	floating with hydroelectric power plants. An analysis of the FPV power potential for the top 20 hydroelectric power plants (HPPs) in the globe reveals that the HPP energy production increases by 65% when 10% of the HPP basin surfaces are covered.	-Numerical analysis - PVsyst software
(Patil et al., 2022)	Studied analysis how the levelized cost of energy enhance by using hybrid floating photovoltaic and hydropower plant at the water dam in Koyana Dam's Shivajisagar . The linked demand is calculated to be 11.26 kWh/day. About 55.60% all of the loads power requirement supply from the grid. The rest 44.4% is from the FPV plant.	-HOMER Pro software
(Taye et al., 2020)	The presented study in Ethiopia's Debre Mariam Island on in Ethiopia. It also compares the efficiency of FPV with traditional land-based PV. This scheme was created to supply the daily energy demand of 1,467.986 kWh for 300 households and public facilities. A ground PV can produce 289.9 kW of power, which of a solar floating system is 294.8 kW. As a result, installing floating PV boosts the output of generated power by 4.9 kW.	-MATLAB/Simulink Software -Numerical floating system modeling -NASA data collected
(Rorisang Christopher Moqulo, 2022)	The study showed the practical, financial and eco-friendly possibility of 7.8 MWp floating solar PV Metolong Dam in Lesotho. It generates 3.4% and 17,345-MWh annual output energy than ground-mounted PV due to the cooling effect of water. The FPV reduces CO_2 emissions	-Microsoft Excel, PVsyst 7.2, PVGIS 5

	by 17,329 tons annually and saves 84,136 m³ of water by lowering evaporation.	
(Kimura et al., 2023)	The Lao PDR dual system, which merging hydroelectric and floatable solar PV in Lao PDR confirmed the system effectively balances seasonal variations. Hydropower performs better in the rainy season, while FSPV generates more electricity during the dry season.	- Satellite-based solar irradiance data for FSPV generation simulation - PV system modeling (module/inverter specs, tilt/azimuth optimization, loss analysis) by using PVsyst.
(Solomin et al., 2021)	Explores the combines method include: floating system with hydropower, wave energy, pumped storage, wind and hydrogen. The paper identified the promising hybrid combination which is FPV and hydro system due to complementary nature and high energy gain.	-Feasibility study
(Nguyen et al., 2023)	In this work, experimentally examined and designed a 47.5 MW grid-connected photovoltaic plant that will be installed on the flotation system at Binh Thuan's Da Mi hydropower reservoir. This was selected to be the first attempt to build a huge-scale floating solar energy system on top of a hydropower basin in Vietnam.	-Experimental analysis -PVsyst software for technical analysis
(Matheus & Musti, 2023)	This paper presented the design and simulation of 5 MW floating solar panel for Goreagab Dam in Namibia. Evaluates technical feasibility, energy output, and financial viability using. Three capacity scenarios (5 MW, 10 MW, and 20 MW) are explored, with the 5 MW system estimated to produce 7.98 GWh annually and reduce water evaporation by 15,000 m^3/year.	- Google SketchUp for 3D modeling and SAM (System Advisor Model) for performance and economic analysis

(Rubens Passos, 2024 n.d.)	This study evaluated the sustainability from technological and financial standpoint integrating a 480MWp floating solar photovoltaic plant with IIha Solteira hydroelectric power plant in Brazil. The result gained is 6% reduction in hydroelectric generation and 7% water saving in turbine due to the integration with FPV.	-MATLAB for mathematical modelling and scenario analysis (wet/dry season, sunny/cloudy/rainy condition) -PVsyst simulated FPV energy output
(Kougias et al., 2016)	Ten dams with an estimated 42 MWp capacity have been chosen, and they should generate 72 GWh of power annually.	-PVGIS tool
(Stiubiener et al., 2020)	The study examine the possibility of switching the solar-hydro model with the corresponding thermal-hydro model. B utilizing 10% of the surface the hydro power reservoirs can support floating photovoltaic delivering demand during high sunlight hours and balancing grid with hydro-power during less light times.	-Feasibility analysis
(Haas et al., 2020)	The storage tank called Rapel, was built in 1968 for energy production which is 75 m long head and generate 380 MW. A storage capacity of 400mm^3 with temperate reservoir. The impact of fractions below 40% on hydropower revenue and microalgae development is negligible or nonexistent. Since less light in the reservoir covers 40% up to 60%, algal blooms are prevented.	-Numerical model that simulates the aquatic bodies of hydrodynamic -hydropower Optimization tool
(Agrawal et al., 2022)	In From India, Rajghat dam in Uttar Pradesh 6513 MWp is calculated to be output from an FPV. The reservoir receives 10,623,501 MWh annually from 25% of its area.	-HOMER pro software

	Every year, 1395 cubic meters of water can be saved per MWp as end value of evaporation. With an internal rate of return (IRR) of 8.55% computed levelized cost of energy (LCOE) is \$0.036/kWh (INR 2.61/kWh). This is encouraging for the widespread use of FPV, which can help safeguard the ownership of agricultural land by solar panels.	
(Mahmood et al., 2021)	In order to take hybrid FPV-hydro systems into consideration, the FPV potential of Australia's four largest hydropower reservoirs is examined. It was predicted that each of the four sites could provide power equivalent to the hydro plant's capacity if an FPV was installed. Less than 15% of the reservoirs' area is used to achieve this. The findings showed that FPV can generate more than 100% of each HPP's installed capacity.	-Feasibility analysis

2.6. What are the research gaps of the above literature review?

Some of the research gaps remained fill under exploration are the influence of specific environmental factors, such as wave action, wind loads, and temperature variations in different geographic regions on the performance and stability of FPV systems. There is limited research on the integration of FPV systems with other renewable energy sources such as wind or hydroelectric power, and how these hybrid systems can enhance overall energy efficiency and reliability. The other gaps are the difficulty of integrating grid system since most researcher was focusing on off grid community.

Despite the increasing adoption of floating solar panel systems as a renewable energy solution, there is a notable deficiency in research focusing on their ecological implications, particularly concerning aquatic life. While numerous studies have explored the efficiency and economic viability of floating solar installations, there is a lack of comprehensive investigations into how these systems may disrupt local aquatic ecosystems, including potential harm to fish populations, plant life, and overall biodiversity.

Nevertheless, almost all of these bifacial research and validation attempts have been carried out on land-based installations with solid ground surfaces, such as gravel, sand, concrete, or grass. There is a noticeable lack of bifacial FPV performance experimentally validated on water surfaces, which differ significantly from solid ground in terms of reflecting characteristics, surface dynamics (waves, ripples), and optical behavior. Bifacial gain factors were measured especially for freshwater reservoirs in tropical regions like Ethiopia, where distinctive reflective conditions are created by high light angles, distinct wet/dry seasons, and changing water clarity.

For water surface verification of the isotropic ground reflection assumption is utilized in Pvsyst for bifacial rear side simulation. The isotropic model of Ineichen et al. (1990) was created and verified for land surfaces rather than water. The highly anisotropic specular reflection (glint) of water is influenced by surface roughness, wind speed, and sun location. Since the majority of previous bifacial studies (Shoukry et al., 2016; Yusufoglu et al., 2015) only provided short-term 5-month validation periods, long-term performance data for bifacial FPV systems on hydropower reservoirs are needed.

Despite these important contributions, no study in the reviewed literature offers an integrated framework for multi-objective optimization that concurrently takes into account. Technical performance (capacity factor, bifacial gain, energy yield, and performance ratio) and economic viability (payback term, internal rate of return, net present value, and LCOE) are not optimize. Benefits to the environment (reduction of CO_2 emissions, conservation of land, and water evaporation) and seasonal matching of solar and water resources is known as hydrological complementarity are not adjust. Costs associated with grid integration (transmission, substation modifications, balancing requirements) is not express in the literatures. Eli Getieas Mandefro & Jember (2022) assessed a 1 MW FPV system on GERD specifically for Ethiopia, but they did not determine the capacity where marginal cost equals marginal gain in order to optimize the FPV capacity based on economic parameters. Since FPV can use the current hydropower transmission lines, calculate the avoided grid infrastructure expenditures. The model does not verify is this the optimal capacity? Could a 50 MWp system provide better economic returns or would a 10 MWp system achieve most of the benefits at lower risk?

No studies in the reviewed literature address the unique ecological context of Ethiopian reservoirs, particularly the GERD. Exley et al. (2022) have shown that placing FPV arrays in faster-flowing areas reduces ecological impact, and Haas et al. (2020) have noted that FPV coverage fractions below 40% have negligible effects on hydropower revenue and micro-algal development, while coverage of 40–60% may actually prevent algal blooms by reducing light penetration. Unlike the temperate reservoirs investigated in Brazil (Moraes et al., 2022), the Blue Nile basin has unique biodiversity, including endemic fish species and aquatic vegetation that may react differently to FPV shade.

Additionally, no ecological study has looked at how FPV mooring systems and related underwater cables affect benthic ecosystems and fish behavior under such dynamic settings, despite GERD experiencing severe annual water level fluctuations ranging from 594.16 m to 623.38 m (a 29.22 m range). High sediment loads are also carried by the Blue Nile, particularly during the rainy season. However, no studies have looked into the long-term biological effects of sediment buildup on floating constructions. Furthermore, Blue Nile flows are crucial to Sudan and downstream communities. Although EliGetieas Mandefro & Jember (2022) discuss water savings for downstream.

Although floating photovoltaic (FPV) systems have been the subject of much research, mono-facial PV modules have been the focus of the great majority of these investigations. The potential benefits of bifacial technology in aquatic contexts are overlooked by this approach. Bifacial floating photovoltaics can capture both direct sunlight and albedo radiation from the water's surface. However they are widely unexplored. The best design, performance characterization, and techno-economic viability of bifacial FPV systems in comparison with the mono-facial counterparts are thus lacking in the literature.

CHAPTER THREE

3. METHODOLOGY

3.1. Research Methodology

Firstly, a case study region is selected the Renaissance Dam in Ethiopia. Wind speed data, solar radiation, and normal ambient temperature are gathered by using Meteonorm 8.1 (2010-2021) from PVsyst software. The floating structural design size a 5.06 MWp FPV system. By comparing two structural designs of FPV evaluate the evaporation rate of the reservoir dam. Then, finding the optimum height, tilt and pitch of the FPV by using PVsyst software. Performance ratio, capacity utilization factor, greenhouse gas emissions, water evaporation, economic analysis, and energy production potential were among the performance metrics of the FPV that were examined. We finish by outlining the advantages, limitations, and future directions of FPV technology in the nation.

3.2. Study Area description

The Nile River flows across the Nile River Basin (NRB) in northeastern Africa from south to north. Ethiopia, the home country of the Blue Nile, has started building the Grand Ethiopian Renaissance Dam (GERD) in 2011, and when it is finished it will produce 6.45 gigawatts of energy (Chen et al., 2021). It is previously known as the Millennium Dam, it is placed in Benishangul Gumuz region 600km northwest of the capital Addis Ababa city and 15km east of the Sudan border. Geographically, the GERD is situated at latitude 11.22°N and longitude 35.10°E. Ethiopia's Grand Renaissance Dam, with a reservoir area of 1,874 km^2 is shown in Figure 3.1. The speed of wind average wind is 3.26 m/s, temperature of 28.38 ºC and, the average global horizontal irradiance is 6.093 $kWh/m^2/day$.

When completed, the Grand Ethiopian Renaissance Dam will have a total volume of 74 Km^3, be 1,800 m long, and be 145 m high, making it the largest dam in Africa. The power plants, which are situated on the river's right and left banks, are made up of 13 Francis turbine units, each of which eleven turbines produce 400 MW and two turbines produce 375 MW of electricity. Together, they have 5,150 MW of installed power and are expected to produce 15,000 GWh annually.

Reservoir details (Di Grazia & Tina, 2024):

- Maximum level of the dam (mean sea level) =640 m
- Normal operation level (mean sea level) = 640 m
- Dead/minimum level (mean sea level) = 590 m
- Total storage capacity = 74 Km^3
- Dead storage capacity=1500 m^3

Figure 3. 1 An overview of the GERD project and water reservoir area (Chen et al., 2021)

Figure 3.2 illustrates the location and geographical feature of the Grand Ethiopian Renaissance dam obtained from google earth.

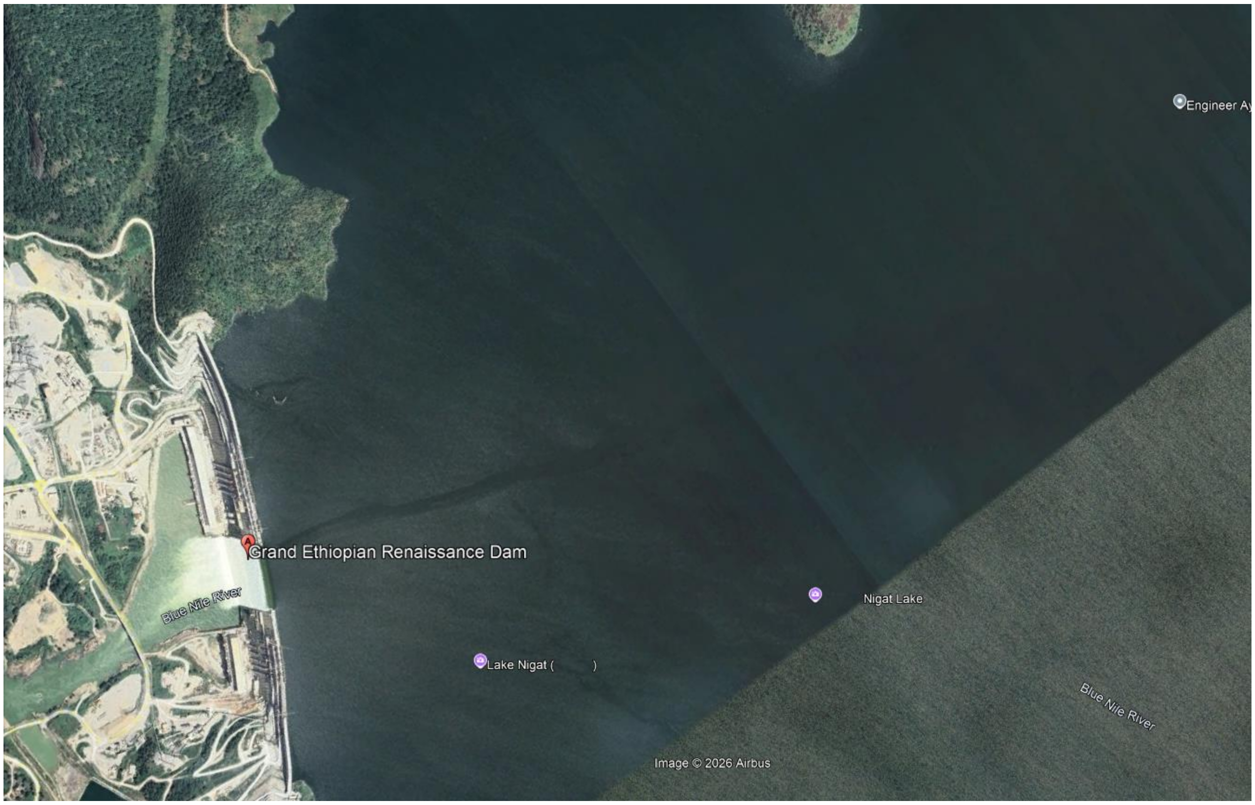

Figure 3. 2 Grand Ethiopian Renaissance Dam from Google Earth

Table 3.1 illustrates the data gained from Meteonorm 8.1 (2010-2021) and NASA/POWER Source Native Resolution Monthly and Annual (2000-2024) during the last ten and twenty-five years.

Table 3. 1. Ethiopian Renaissance Dam metrological information

Months	Global horizontal irradiation (kWh/m^2/day)	Wind Speed (m/s) at 2 Meters	Temperature (°C)
January	6.36	3.46	26.99
February	6.27	3.69	29.33
March	7.08	3.70	31.97
April	7.147	3.75	32.60
May	6.37	3.54	31.42
June	5.67	3.48	28.03
July	5.197	3.39	26.30
August	5.17	3.17	25.10
September	5.50	2.76	25.26
October	5.9	2.42	27.20

November	6.3	2.70	28.88
December	6.17	3.05	27.60
Annual Average	6.093	3.26	28.38

The produced power supply to the grid by two types of transformers. Those are step up transformer and step-down transformer.

1. Step up transformer: 18kv step up to 500kv main line to Holeta and 400kv to Addis Ababa
2. Step down transformer: 18kv step down to 15kv and 15kv step down to 400v

3.3. FPV installation Location

As we known, the site is next to the powerhouse side of the Grand Ethiopian Renaissance Dam. The lack of mountains in that area helps in avoiding the shadows that the mountains cast. The FPV structure has a walkway that helps in maintenance, and because it is close to a dry area, it is easy and affordable to tie the FPV.

The location is near to the powerhouse of hydroelectricity reservoir for their ability in the utilizing the existing grids and power management for day and night. The FPV panel, near place around the dam and not covered by mountains is shown as a Figure 3.3 and Figure 3.4. There is an abundant solar radiation and wind speed less than 5 m/s.

From this closed area, 2.3% of 1 Km^2 is taken as FPV covered area. It is 23,000 m^2 total and considering FPV structural design for walk way and pitch as 7%, then the area taken is 21,390 m^2.

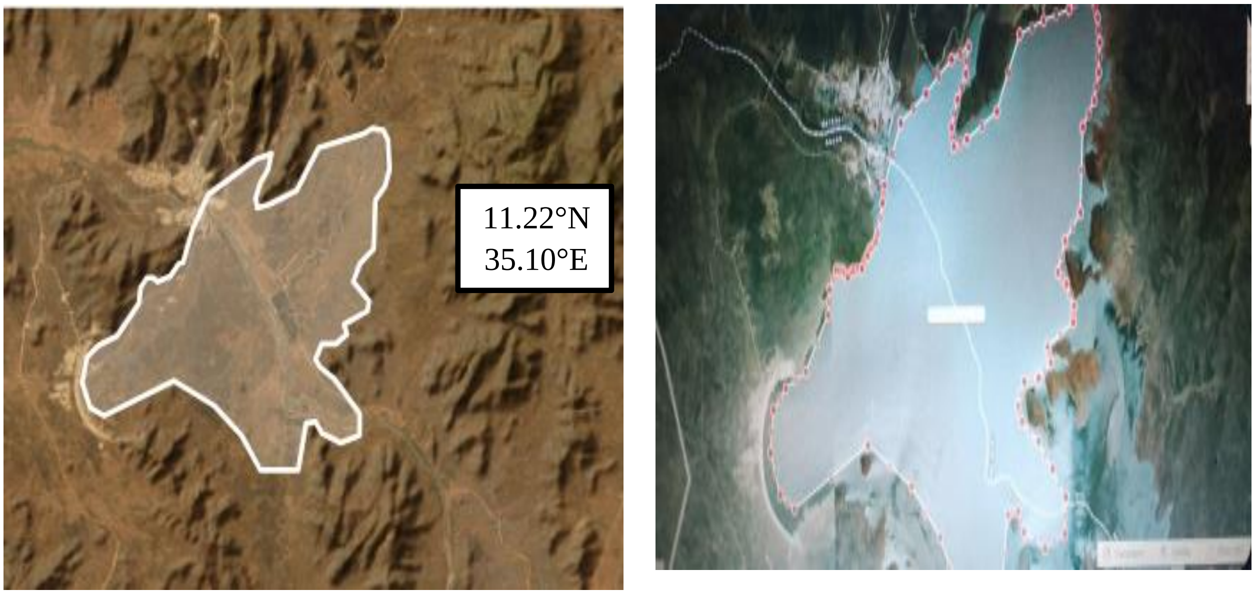

Figure 3. 3 Reservoir of the Grand Ethiopian Renaissance Dam 11.22°N and longitude 35.10°E

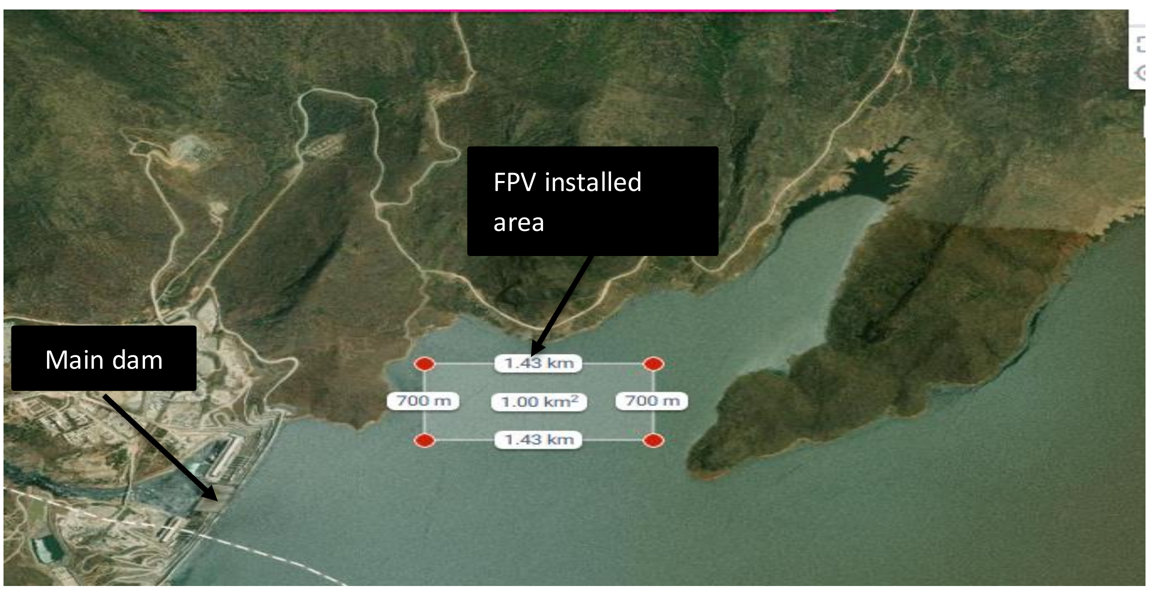

Figure 3. 4 Selected area to install FPV panel

3.4. Main Structural component of FPV

An FPV system consists of several components, depending on various parameters. The most common components are listed below (*Structural FPV*, n.d.):

1. Photovoltaic panel along with additional electrical conditioning equipment to generate electricity from solar radiation.

2. A Floating Structure or pontoon that allows and supports the installation of PV module while maintaining buoyancy.
3. Mooring system and buoyancy anchors which can adjust to fluctuating water levels despite the fact preserving its spot.
4. Underground cables to transmit the power produced from FPV system to land. Generated electricity can either be fed into the grid or stored in forms of batteries.

Table 3. 2 Floating PV structure

Structural type	Descriptions	pros	cons	Useful for
HDPE Modular Pontoon(Plastic)	Every panel or set of panels is supported by floating plastic components that interlock.	Low cost, simple to install and move, low maintenance, and resistant to corrosion and UV rays.	Low strength for harsh waves (>1-1.5m), risks overturning.	Calm inland reservoirs/lakes
HDPE float with metal frame (Galvanized steel frame)	Floats provide buoyancy, while a rigid frame holds the PV modules	Added rigidity, optimal angles, higher capacity	Metal corrosion risk if not protected, heavier, expensive than pontoon only	Moderate waves, larger farms needing
Semi-submersible structure	Submerged pontoons/columns with elevated deck	High stability in 5-6m waves,	High expensive, complex assembly	Offshore/marine
Tracking FPV structure(moving mechanism)	Panel rotate or track the sun while floating	Higher energy yield	Very expensive, more maintenance, more moving parts	only if budget is high and Operation & Maintenance is strong

For the Grand Ethiopian Renaissance Dam (GERD) from Table 3.2, the HDPE modular pontoon system in combination with an aluminum or galvanized steel support frame is thought to be the best choice among the existing floating photovoltaic structural designs. Good buoyancy, corrosion resistance, modularity, ease of installation, low maintenance, and affordability are all provided by this structure. It is particularly suitable for inland bodies of water with a lot of surface area and very mild wave conditions.

The structure is designed to hold the panels at an optimal angle of 20° as shown in Figure 3.5 with white reflectors concentrate the solar radiation.

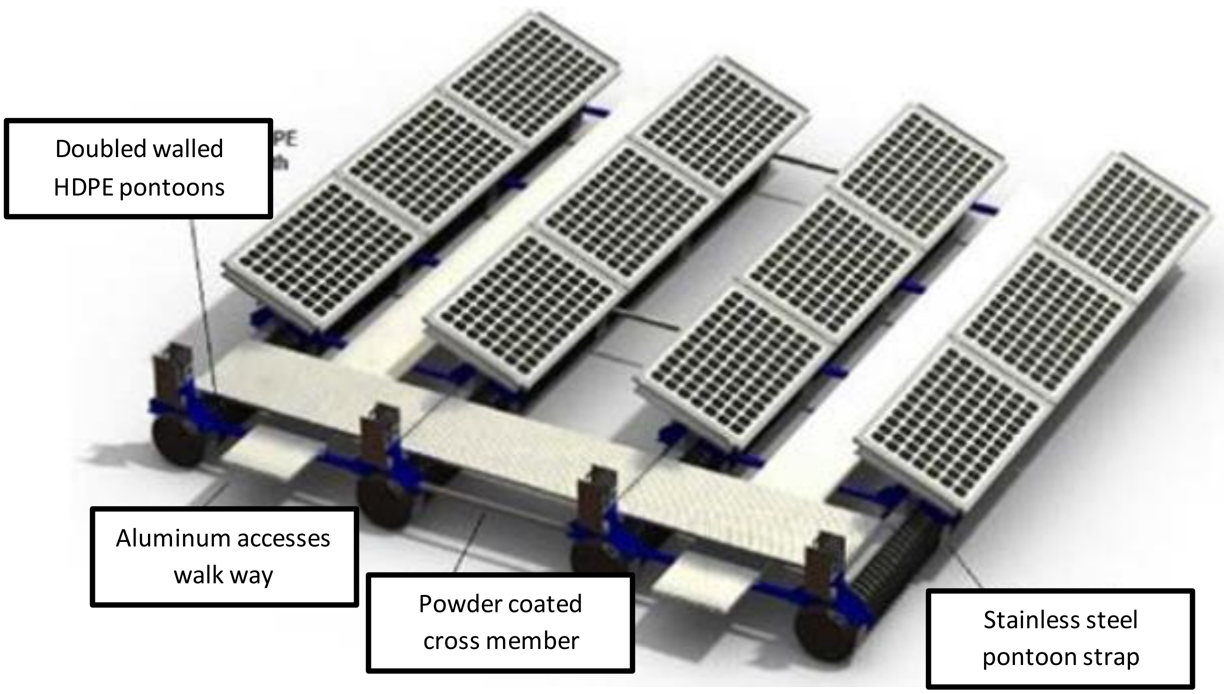

Figure 3. 5 Designed FPV with walkways (Asmy & Arshad.,2020)

3.4.1. Depth of the water body

Depth of the waterbody is also an important parameter in designing of FPV plants. According to (MARCO ROSA-CLOT, 2018) with the increasing depth, the length of the mooring or anchoring cable will also increase.

Since the maximum recorded water depth is 623.38 and the minimum water depth is 594.16 the cable length of the pontoon up to land surround it to anchor the cable is 29.22m.

Table 3. 3. GERD water level and yearly discharge of the water (2023)

Date	Water level (m)	Q discharge (m/s)
January	599.8	395.66
February	596.03	220.28
March	594.67	377.65
April	594.16	180.76
May	594.61	691.79
June	595.12	1456.69
July	599.86	4137.84
August	612.29	5614.91
September	621.27	4690.19
October	623.38	2232.58
November	622.27	2251.7
December	619.93	847.32
max	623.38	5614.91
min	594.16	180.76

3.5. Sizing Solar Photovoltaic

i. Solar Photovoltaic

The sizing of the floating solar photovoltaic system for 5.06 MWp power generation was conducted by selecting the 72-cell solar PV panel of 440Wp power output of panel ($\mathrm{P_{panel}}$) to balance the efficiency and lower cost (Nguyen et al., 2023) and Table 3.4 shows the specification of the selected PV cell. The number of panels (N) required in GERD to generate the design maximum power ($\mathrm{P_{max}}$) of 5.06 MWp was evaluated using Equation (3.1) (EliGetieas Mandefro & Jember, 2022) below.

$$N = \frac{\mathrm{P_{max}}}{\mathrm{P_{panel}}} \qquad 3.1$$

$$N = \frac{5060000}{440} = 11500\ units$$

The total installation area available ($\mathrm{A_{ava}}$) for the floating PV system is calculated using Equation (3.2) based on multiplying the single panel area ($\mathrm{A_{on}}$) of 2 m^2 with the required total number of panels (N_{mod}) of 11,500 is calculated to be 23,000 m^2 which is under the design total area over the GERD.

$$A_{ava} > N_{mod} \times A_{on} \quad 3.2$$

Table 3. 4. PV panel characteristics

Model	Mono 440 Wp 72 cells bifacial
Maximum power (Ppeak)	440 W
Voltage of open circuit (Voc)	49.80 V
Current in short circuit (Isc)	11.10 A
Maximum power point voltage (Vmpp)	41.10 V
Maximum power point current (Impp)	10.780 A
Efficiency	19.66 %
Coefficient of tem Pmax (%)	-0.36 %/°C
Coefficient of tem Voc (%)	0.144 % V/°C
Coefficient of tem Isc (%)	+0.046 % A/°C
Bifaciality factors	80%

ii. Inverter

An inverter for the GERD floating PV system to convert the DC power output of floating PV system into an AC power that is suitable for grid connection is selected based on the total solar PV power P_{DC} output of 5.06 MWp and inverter side DC/AC ratio of between 1.15 to 1.3 (Matheus & Musti, 2023), where in this study a value of 1.227 is selected and the total inverter power output (P_{AC}) of GERD floating PV system inverter is evaluated using Equation (3.3). Once the total inverter power is calculated, a string type inverter is selected due to its flexible to be integrated in different strings floating photovoltaic system over the GERD and the detail specification of the selected inverter is presented in Table 3.5.

$$P_{AC} = \frac{P_{DC}}{\frac{DC}{AC}} \quad 3.3$$

$$P_{AC} = \frac{5.06}{1.227} = 4.12 \text{ MW ac}$$

Table 3. 5. Inverter specification

Model	Huawei Sun2000-330,Sunway SKID 2700-620
Rated power DC	24 kw
Imppt	240 A
Isc	199 A
Vmppt Dc	500-1500 V
Efficiency	98.9 %
Rated power AC	257-4125 kWac
Output	50/60 Hz, 800 V ac

3.6. FPV System Mathematical Model

In modeling the floating photoelectric system over the GERD the power generated by the system, the amount of water saved and the performance ration of the system was calculated in the following section.

3.6.1. Analysis of solar photovoltaic

The amount of solar radiation on the floating tilted surface (I_T) over the GERD is evaluated by adding the beam (I_b), diffused (I_d) and reflected (I_r) flux over the tilted floating surface with their corresponding tilt factors using Equation (3.4) (Pakyala, 2021).

$$I_T = I_b r_b + I_d r_d + (I_b + I_d) r_r \quad 3.4$$

Where: r_b is the beam radiation tilt factor,

r_d is the diffused radiation tilt factor, and

r_r is the reflected radiation tilt factor.

The water temperature is calculated using the relation with the air temperature using Equation (3.5) and the wind velocity over the GERD water surface is calculated using Equation (3.6).

$$T_w = 5 + 0.75\ T_a \quad 3.5$$

$$\mathrm{V_W} = 1.62 + (1.62\ \times\ V_{Land}) \quad 3.6$$

In PVSYST software the value of the loss of heat factor (u-value) and albedo for floating solar panels will be adjusted to the recommended value of 0.2 (MARCO ROSA-CLOT, 2018) for albedo at the water surface and 32 W/ ($m^2 \cdot K$) for the U-value.

In a solar floating system, the PV cell's temperature is determined using Equation (3.7):

$$T_P = 0.943T_w + 0.0195G - 1.528V_w + 0.3529 \qquad 3.7$$

Where T_P and T_w are the FPV cell temperature and temperature of the water respectively in degrees Celsius, G is the average daily irradiance (W/m^2), and V_w is the wind velocity over the water's surface (m/s).

3.6.2. PV array-produced electrical energy

The DC daily energy output ($\boldsymbol{E_d}$) of floating photovoltaic system over the dam is evaluated using Equation (3.7) by using the transmitted irradiance on the cell ($\boldsymbol{I_{tr}}$) by the DC capacity of the cell ($\boldsymbol{P_{dc}}$) and the monthly energy output ($\boldsymbol{E_m}$) is evaluated by multiplying by the daily energy output by total number of the days ($\boldsymbol{N}$) in that production month using Equation (3.8) (Pakyala, 2021).

$$E_d = (I_{tr/1000}) \times (P_{dc}) \times (1 + \gamma(T_{ce} - T_r)) \qquad 3.8$$

$$E_m = (E_d) \times N \qquad 3.9$$

Where: T_{ce} = temperature cell,

γ = coefficient of temperature, which is -0.0047/°C, and

T_r = 25°C is the reference cell temperature

The total AC energy output of the FPV (E_F) system and integrated with an inverter of efficiency 98.9 and supplied to the grid (E_g) are evaluated using Equation (3.10) and Equation (3.11) respectively (Chico Hermanu et al., 2019; Pakyala, 2021).

$$E_F = E_{dc}[(1 - L\,\%)] \qquad 3.10$$

$$E_g = E_F[1 - (L_i\,\% + L_{ca}\,\%)] \qquad 3.11$$

3.6.3. Capacity consumption rate and yearly performance ratio

The performance of the floating photovoltaic system over the GERD is evaluated by the performance ratio (PR) where the ratio of the energy supplied to the grid (E_g) by the rated power

(P_o) of the system to the ratio of the irradiance (I_{tr}) by the standard irradiance (I_o) of 1000 W/m^2 as shown in Equation (3.15) (Pakyala, 2021).

Final (useful) Yield, the AC energy delivered normalized to rated capacity:

$$Y_F = \frac{E_g}{P_o}\ (KWh/KWp) \qquad 3.12$$

Array Yield the DC energy production normalized to the rated capacity:

$$Y_A = \frac{E_d}{P_o} \qquad 3.13$$

Reference Yield, the equivalent full-sun hours available at the site equ(3.14):

$$Y_R = \frac{I_{tr}}{I_o}\ (KWh/KWp) \qquad 3.14$$

Performance Ratio, the overall system efficiency accounting for all losses equ(3.15):

$$PR = \frac{E_g/P_o}{I_{tr}/I_o} \qquad 3.15$$

Equation (3.16) provides the formula for the yearly capacity utilization factor (CUF), which is the ratio of actual energy generated to a power plant's theoretical maximum energy production.

$$CuF = \frac{E_g}{24 \times 365 \times P_o} \qquad 3.16$$

3.7. Reduction in Evaporation

A significant decrease in evaporation from the water surface covered by the pontoon supporting the PV modules is a byproduct of the FPV plant. Features of the floating PV array may have distinct effects on the energy balance of the covered portion of the basin and water evaporation. The study's findings demonstrate that evaporation may be decreased from 6 to 18% by covering just 10% of the water's surface. Modules in floating systems that are attached to a tubular buoyancy system provide more ventilation, which improves evaporative cooling.

The rate of evaporation that results from installing various FPV topologies on the reservoir. It is possible to emphasize that the features of floating systems as well as the proportion of surface covered determine how much water evaporates (Bontempo Scavo et al., 2021). Covering only 30% of the surface of a reservoir, it is possible to obtain up to 49% reduction in evaporation.

An initial examination of the various FPV plant typologies is necessary for the investigation of evaporation in the presence of floating PV systems in water. The primary factor influencing water evaporation is the solar radiation (direct and/or diffuse component) that strikes the water's surface; as a result, it is critical to determine how and to what extent the contribution of solar radiation changes with installation typologies. Sahu et al. wrote different installation solutions (Sahu et al., 2016), which are classified as follows:

i. Small footprint FPV

Figure 3.6 shows floating systems with modules fastened to a tubular buoyancy system. Because the water in the basin naturally evaporates, these systems enable adequate cooling and ventilation of the modules. The modules may function at lower temperatures thanks to this type of installation, which boosts their efficiency (Bontempo Scavo et al., 2021). Because the PV modules are hanging and the buoyancy structure only covers a portion of the water's surface, solar radiation transmission through the water's surface is decreased but not entirely halted.

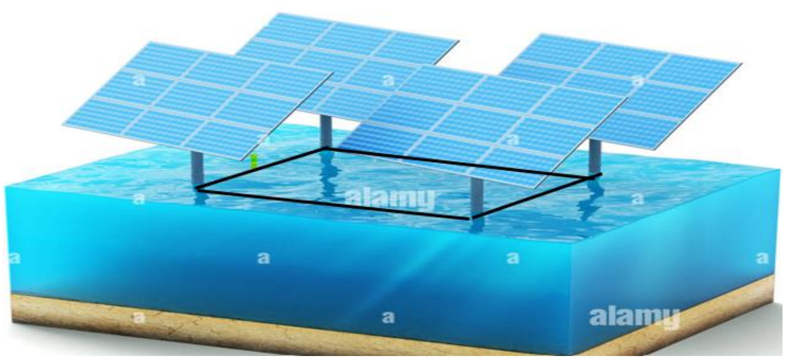

Figure 3. 6 Modules coupled to a floating system

ii. Large footprint FPV

Figure 3.7 shows floating systems with floats covering the whole surface beneath the module. Modular floating platforms made of polyethylene that are secured to the ground by elastomers make up the system. This enables more adaptability in the case of a significant and abrupt change in the water level (Bontempo Scavo et al., 2021). Because the platforms are designed to totally cover the underlying surface, there is very little solar radiation transfer underneath them.

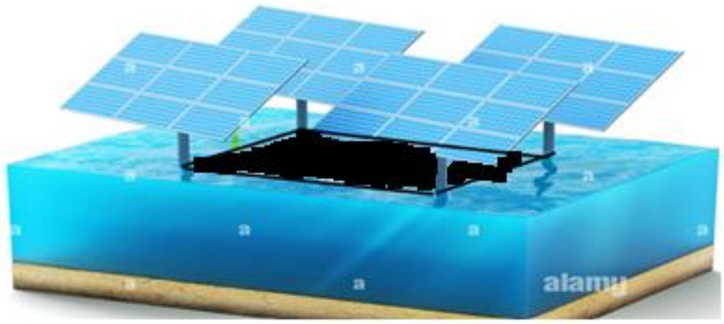

Figure 3. 7 The area beneath the module is completely covered by the floats

Water evaporation from the irrigation reservoir was estimated using the well-established Penman equation 3.17 (Valiantzas, 2006): -

$$E_F = \frac{\Delta}{\Delta+\gamma}\frac{R_n}{\lambda} + \frac{\gamma}{\Delta+\gamma}\frac{6.43(f_u)D}{\lambda} \qquad 3.\ 17$$

Where: E_F is potential open water evaporation or evapotranspiration (mm/d),

R_n is net radiation at the surface (MJ/m^2/d),

The term R_n in equation 3.18 is calculated using the following equations:

$$R_n = SW_n + LW_n \qquad 3.\ 18$$

$$SW_n = (1-\alpha)(R_d + R_b) \qquad 3.\ 19$$

$$LW_n = \sigma T_w^4\,(0.56 - 0.0092\sqrt{e_a})(0.1 + 0.9c) \qquad 3.\ 20$$

$$e_{a=}\ 0.5(\frac{RH}{100}(es(Tmax) + es(Tmin)) \qquad 3.\ 21$$

Where in (Farrar et al., 2022) R_d and R_b are the diffuse horizontal irradiation and direct beam radiation in MJ/m^2/day respectively, α is the absorptivity of the Earth's atmosphere, taken to be 0.3, SW_n and LW_n are the net incoming short wavelength radiation and long wavelength radiation in MJ/m^2/day respectively, σ is the Stefan-Boltzmann constant, 5.67x10-8 W/m^2/°C^4 and c is the cloudiness index (Farrar et al., 2022), e_a is mean daily Vapor pressure. The maximum and minimum temperature of the given site in °C are $es(Tmax)$ and $es(Tmin)$ respectively. For simplification, the summation of R_d and R_b in equation (3.19) was taken to be equivalent to the global horizontal irradiation, R_{GHI}. This assumption has limited impacts on the results of the calculation (Farrar et al., 2022).

For small footprint in figure 3.6:

Since there is no full contact with the water surface, they protect it from direct beam radiation but not diffuse radiation (Farrar et al., 2022). Hence, shortwave radiation is modified to only include the diffuse component in equation 3.22 of the solar radiation as shown:

$$SW_n = (1-\alpha)R_d \quad 3.22$$

$$R_d = K_d \times R_{GHI} \quad 3.23$$

$$K_d = 0.847 - 0.985c \quad 3.24$$

Where K_d is the diffuse fraction of the global horizontal radiation, it is calculated from the above empirical Equation for Amman, Jordan (Hijazin, 1998).

Longwave radiation for small footprint FPV equation (3.25) modified as cloudiness (C) =0.3 and can be calculated as:

$$LW_n = \sigma\, Tw^4\,(0.56 - 0.0092\sqrt{e_a})(0.1 + 0.9 * 0.3) \quad 3.25$$

For Large footprint in figure 3.7:

Negligible shortwave solar radiation hit the surface of the reservoir. As a result, the equations are modified to:

$$SW_n = 0 \quad 3.26$$

$$LW_n = 0.1\sigma T_w^4\left(0.56 - 0.0092\sqrt{e_a}\right) \quad 3.27$$

Where: $e_s(T)$ is saturation vapor pressure at ambient temperature T in °C, the slope of the saturation vapor pressure curve Δ (kPa/°C) in equation (3.28), λ is latent heat of vaporization (MJ/kg) in equation (3.30), γ is psychrometric coefficient (kPa/°C) in equation (3.31), p is atmospheric pressure (Kpa) and Z is elevation (m) in equation (3.32).

$$\Delta = \frac{4098 \times \mathrm{es(T)}}{(T+237.3)^2} \quad 3.28$$

$$e_s(T) = 0.611\ exp\left(\frac{17.2 \times T}{T+237.3}\right) \qquad 3.29$$

$$\lambda = 2.501 - (2.361 * 10^{-3})\ x\ T \qquad 3.30$$

$$\gamma = 0.0016286 \times \frac{p}{\lambda} \qquad 3.31$$

$$p = 101.3\ \times \left(\frac{293-0.0065 \times Z}{293}\right)^{5.26} \qquad 3.32$$

Where, f_u is wind function in (m/s), a_u and b_u are wind function coefficients, for the original Penman (1948, 1963) equation 3.33, a_u = 1, b_u = 0.536, U is wind speed at 2 m height (m/s) (Valiantzas, 2006).

$$f_u = a_u + b_u U \qquad 3.33$$

D in equation 3.34 is vapor pressure deficit (kPa), e_s is saturation vapor pressure (kPa), e_a is actual vapor pressure (KPa).

$$D = (e_s - e_a) \qquad 3.34$$

Since e_s is not a linear function of temperature, (Valiantzas, 2006) recommended equation 3.35 to compute the mean vapor pressure deficit,

$$D_{(av)} = e_{s(av)} \left(1 - \frac{RH}{100}\right) \qquad 3.35$$

Where $e_{s(av)}$ is mean saturation vapor pressure for the examined time interval estimated as:

$$e_{s(av)} = 0.5[e_s(T_{max}) + e_s(T_{min})] \qquad 3.36$$

Where: $e_s(T_{max})\ and\ e_s(T_{min})$ are saturated vapor pressures corresponding to the temperature values of T_{max} and T_{min}, respectively, and RH is mean relative humidity for the examined time interval. The final equation to find the evaporation reduced by using small (E_{FS}) and large footprint (E_{FL}) are given in equation 3.37 and 3.38.

$$E_{FS} = E_F\ (1 - x) + xE_s \qquad 3.37$$

$$E_{FL} = (1 - x)E_F \qquad 3.38$$

3.8. Economic Analysis of the system

PVsyst provides several financial parameters to assist with the economic assessment of a PV system. PVsyst uses parameters to calculate key economic indicators, such as the Net Present Values (NPV), Internal Rate of Return (IRR), Payback Period, and Levelized Cost of Energy

(LOCE) (Dellosa et al., 2024). These indicators can help decision-makers assess the financial viability of the research.

$$NPV = \sum_{t=1}^{n} \frac{C_t}{(1+r)^t} - C_0 \quad 3.39$$

Where: C_t is the net cash inflow during the period t, r is the discount rate (expressed as a decimal), t is the number of time periods, n is total number of periods and C_0 is the initial investment.

Internal Rate of Return, the discount rate at which NPV equals zero:

$$0 = \sum_{t=1}^{n} \frac{C_t}{(1+IRR)^t} - C_0 \quad 3.40$$

Capital Recovery Factor (CRF) calculated as:

$$CRF = \frac{r(1+r)^n}{(1+r)^n - 1} \quad 3.41$$

Levelized Cost of Energy: $$LCOE = \frac{\sum \frac{(C_t + M_t + F_t)}{(1+r)^t}}{\sum \frac{E_t}{(1+r)^t}} \quad 3.42$$

Where C_t is the capitalized expenditures in the year t, M_t is the operation and maintenance expenditures in the ears t, F_t is the fuel expenditure in the year t, and E_t is the electricity generation in the year t.

3.9. Optimization of FPV system

The system optimization process made use of the PVSYST embedded algorithm. The tilt angle, height, pitch angle which will be used are listed in the table below. The goal is to maximize the energy that is added to the grid. Using tilt angel 20°, pitch distance 1m and height 0.5m increase the supplied energy.

Table 3. 6 Optimization of tilt, pitch and height

Tilt Angel (°)	Pitch Distance (m)	Height (m)
15	0.5	0
20	1	0.5
25	1.5	0.75

30	2	1

CHAPTER FOUR

4. RESULT AND DISCUSSION

In this work, the PVSyst program was used to simulate the design and analysis of an on-grid solar PV system. The most welcoming results were found and reviewed in the results analysis section after numerous simulations runs and calibrations. The model should be simulated following the previously outlined design procedure, and the results can be analyzed to determine plant efficiency. A comprehensive simulation has been conducted to gain a better knowledge of the installed plant, and several results have been produced.

Here are a few various outcomes, including daily input/output plots, a snaky diagram depicting losses, a performance ratio data plot, a daily energy output plot with incident variations, a plot of the chosen location drawn by the horizon line, a plot of the array temperature under operating conditions, a plot of the array power distribution, normalized productions with loss changes, and a plot looking at the sun azimuth and incidence angle, respectively.

4.1. PVsyst Result

In addition to variables such as the global irradiance incidence in the collector plane, the ambient average temperature, the horizontal global irradiance, and the effective global irradiance following soiling losses Table 4.1 displays the balance values and important discoveries. In addition to these variables, the DC energy produced by the poly crystalline bifacial solar array, the energy injected into the grid after taking photovoltaic array losses into account, electrical components, and system efficiency were all simulated. The variables may have annual values, such as summations for energy and irradiance and averages for temperature and efficiency.

According to PVSyst software, the floating bifacial photovoltaic module can provide around 9183192 KWh of power annually, regardless of the size and configuration of the solar panels. The system's performance ratio (PR) is 80.2%.

Table 4. 1.Incident global radiation (GlobInc annually) and generated energy in array and energy injected to grid.

Months	Global hori(kWh/m^2/day)	GlobHor (kWh/m^2/month)	GlobInc (kWh/m^2)	E_Array (kWh)	E_Grid (kWh)	PR ratio
January	6.36	190.8	219.3	934354	905309	0.802
February	6.27	188.1	204.4	861901	835,022	0.795
March	7.08	212.4	215.1	904730	877,072	0.789
April	7.147	214.4	200.6	846419	820,735	0.79
May	6.37	189.8	167.5	718468	696,710	0.798
June	5.67	170.0	146.4	640298	620,640	0.811
July	5.197	155.9	137.2	606124	587,488	0.818
August	5.17	155.2	141.0	621444	602,108	0.817
September	5.50	165.1	159.5	698059	676,624	0.816
October	5.9	177.1	184.4	795,893	771,560	0.808
November	6.3	189.2	215.4	913,232	885,165	0.796
December	6.17	185.6	219.1	933,483	904,757	0.798
Years	6.093	2193.5	2209.9	9,474,405	9,183,192	**0.802**

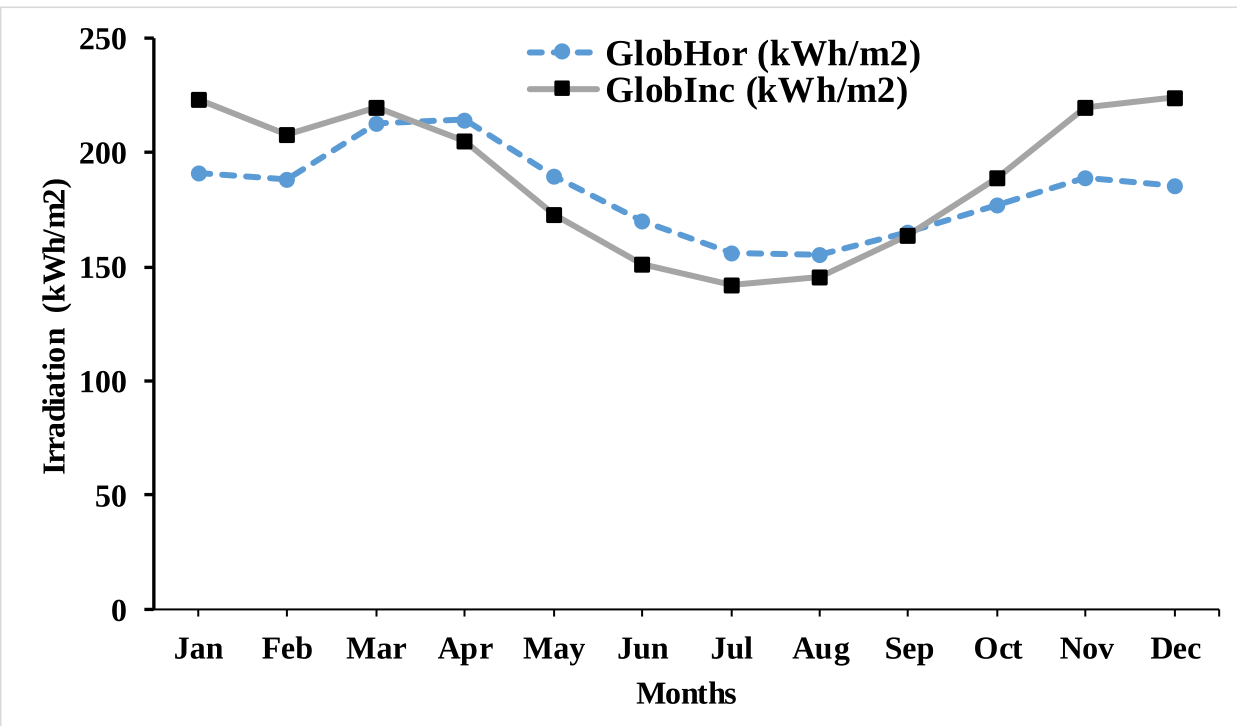

Figure 4. 1 Global horizontal and global inclination, radiation on the panel

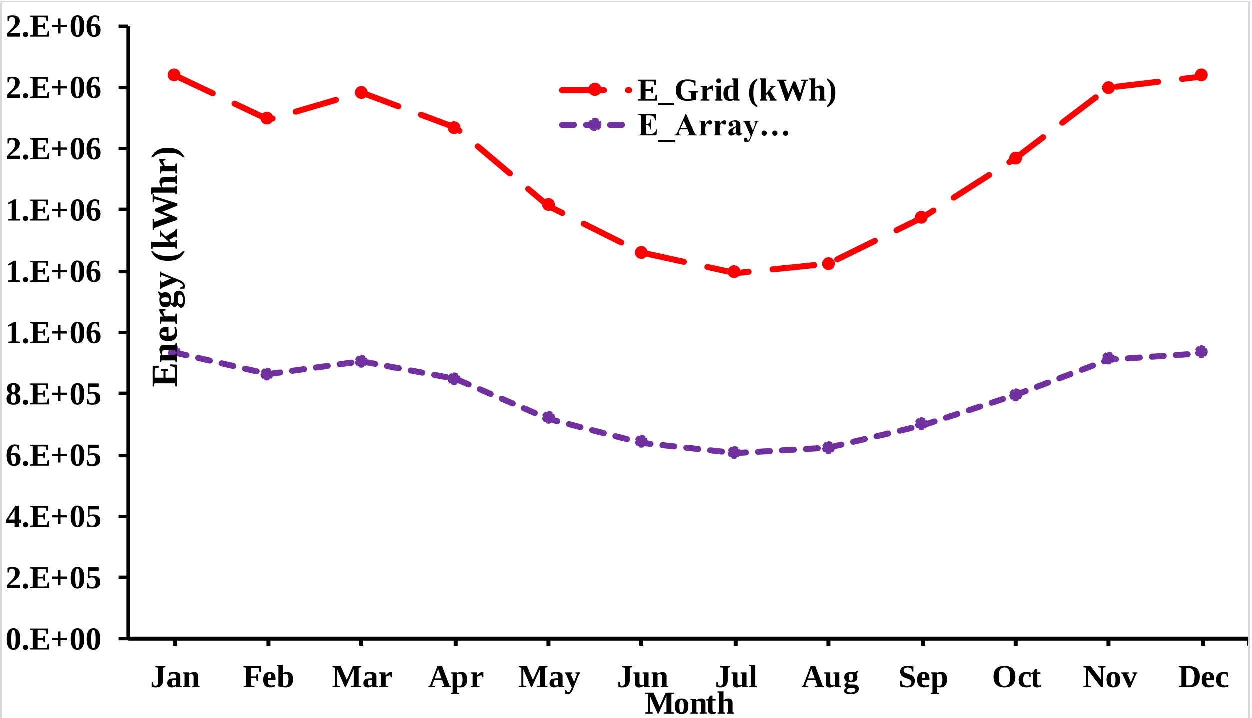

Figure 4. 2 Energy of the Array and Energy of the Grid Vs Months

Based on the PVsyst simulation result and the post electricity generation in 2023 Table 4.1 shows the monthly average electricity production of floating photovoltaic system, GERD hydropower plant and hybrid system from January to December.

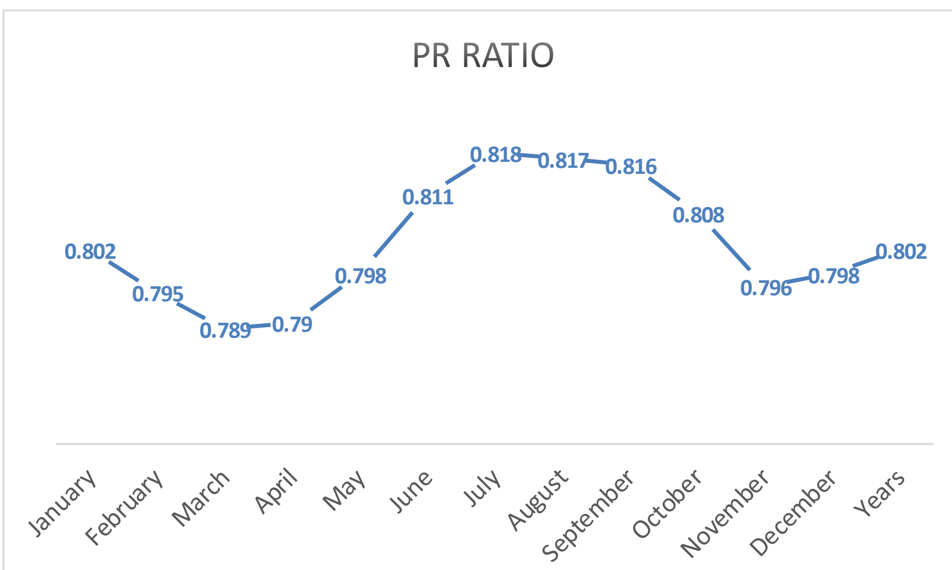

Figure 4. 3 Monthly performance ratio of FPV

Grand Ethiopian renaissance Dam energy production along the year 2023 and 2024 is recorded from Ethiopian electric power.

Hybrid Floating – Hydro energy production (in kWh GERD) 2015 E.C

Table 4. 2. Monthly Average Electricity Production of FSPV, GERD Hydro (2023 data), and Hybrid

Months	E-Grid (FPV) kWhr	E-Grid (Hydro) kWhr	Total Energy
January	905309	63,441,730.00	64,347,039.00
February	835,022	72,468,000.00	73,303,022
March	877,072	70,634,700.00	71,511,772.00
April	820,735	0	820,735
May	696,710	66,600,900.00	67,297,610.00
June	620,640	212,020,200.00	212,640,840
July	587,488	114,990,300.00	115,577,788.00
August	602,108	166,120,200.00	166,722,308
September	676,624	20,814,330.00	21,490,954.00
October	771,560	108,375,300.00	109,146,860
November	885,165	121,119,300.00	122,004,465.00
December	904,757	114,242,000.00	115,146,757
Year	9,183,192	1,130,826,960.00	1,140,010,150.00

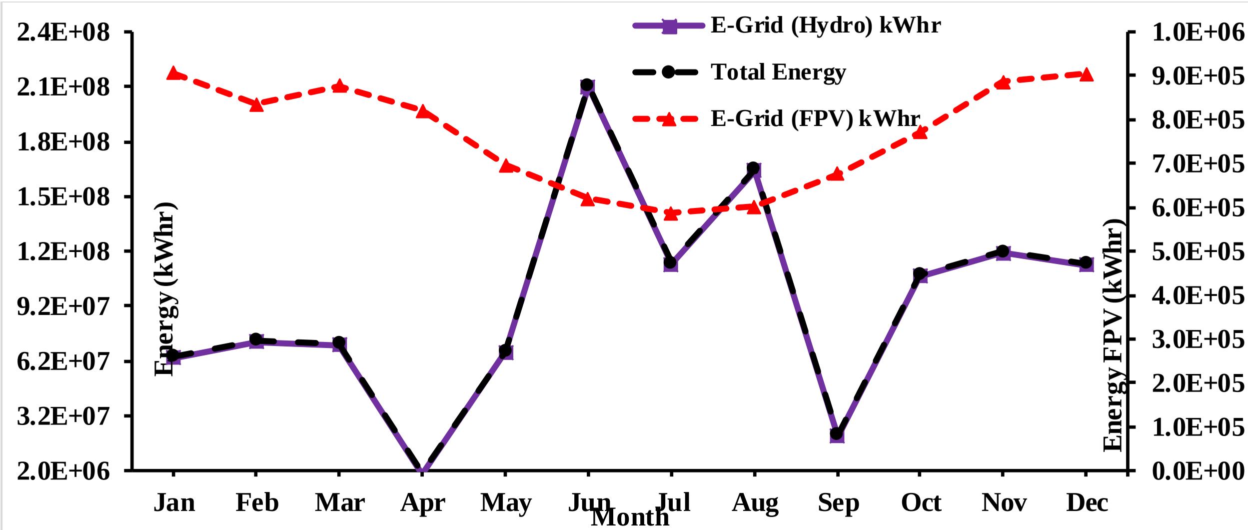

Figure 4. 4 Monthly Average Electricity Production of FSPV, GERD Hydro (2023 data), and Hybrid

The FPV system add extra energy to the hydropower system. To calculate the percentage of total energy comes from FPV:

$$E_{PV} = \frac{E_{PV}}{E_T} \times 100\% = \frac{9{,}183{,}192}{1{,}140{,}010{,}150} \times 100\% = 0.08\%$$

$$E_H = \frac{E_H}{E_T} \times 100\% = \frac{1130826960}{1{,}140{,}010{,}150} \times 100\% = 99.19\%$$

The proposed floating photovoltaic (FPV) system adds more electrical energy to the reservoir's current hydropower producing profile, according to the monthly energy output figures. The hydropower system produced 1,131.828 GWh and the FPV system produced 9.183 GWh annually, for a total hybrid annual energy production of 1,140.010 GWh. This indicates that the FPV system accounts for about 0.08% of the annual hybrid generation. Thus, the combination of FPV and hydropower increases the reservoir's overall energy productivity while using the same water surface area for two different types of energy output.

4.2. Performance Ratio

The primary purpose of the performance ratio (PR) is to assess a FPV plant's quality. It clarifies the connection between the FPV system's theoretical and real energy production. After subtracting all energy use and losses, the PR displays the energy. Because of the unavoidable losses that happen during operation, the PR is normally about 80.02%. The PV plant's PR, or annual average

PR value, is shown in figure 4.5. The PR value fluctuates slightly each month, as shown in the figure.

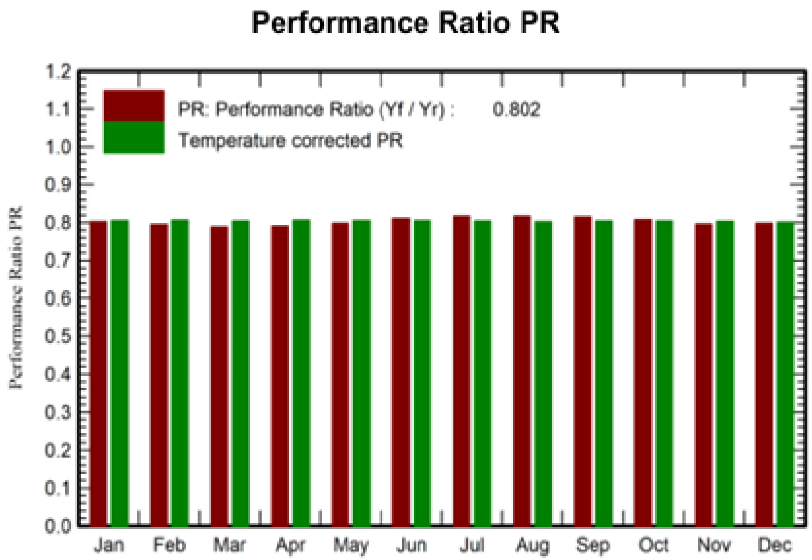

Figure 4. 5 Performance ratio (PR)

4.3. Normalized Productions

The FPV power plant's normalized production is shown in figure 4.6. It displays FPV array collecting losses, large inverter outputs, and system losses. There is a clear depiction of the monthly usable energy output and losses per kWh. These normalized products and standard variables for assessing the performance of FPV systems are established under the IEC rules. The FPV array capture or collecting losses are 1.07 kWh/kWp/day. The system loss is 0.16 kWh/kWp/day, whereas the solar energy output is 4.97 kWh/kWp/day.

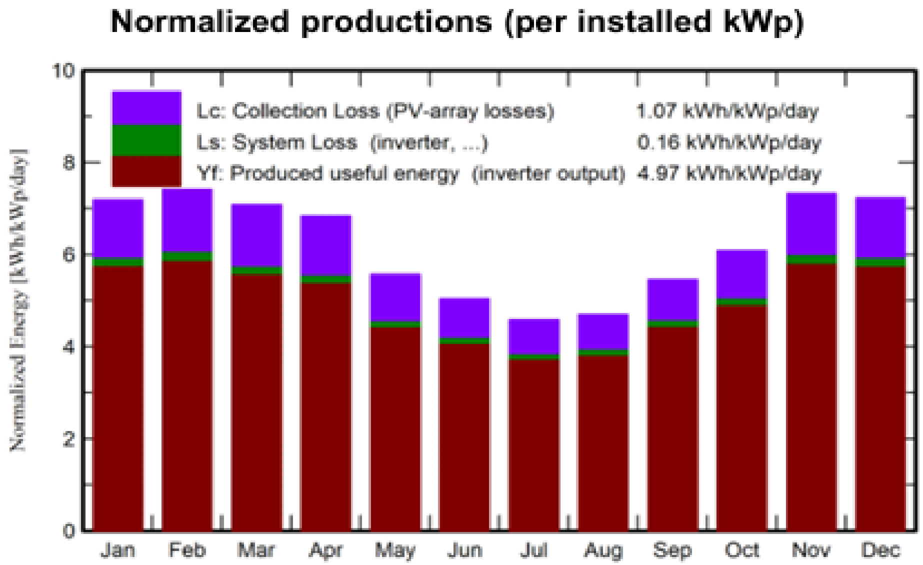

Figure 4. 6 Normalized production (per installed capacity kWp)

4.4. Array Loss Diagram

Computer simulations, which aid in the investigation of various losses that may occur during the installation of PV plants, are used to create the array loss diagram. Figure 4.7 displays the array loss diagram, which illustrates the various losses in the system. The horizontal plane's global radiation is 2193 kWh/m^2. However, the collector's effective irradiance is 2210 kWh/m^2. This near shad irradiance loss is 1.25.

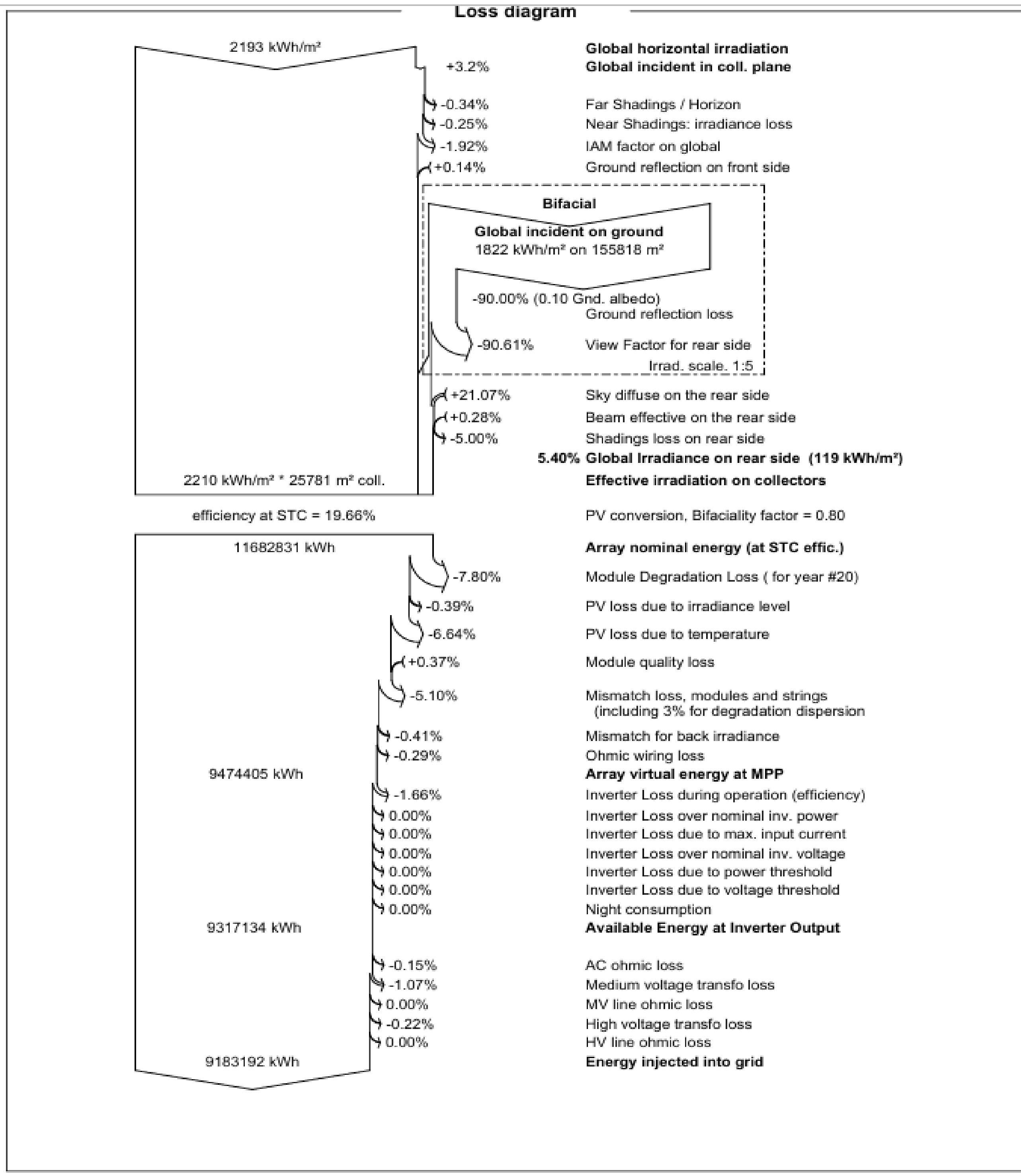

Figure 4. 7 Array Loss Diagram

Electricity or electrical energy is produced when the surface of a photovoltaic module or array is exposed to this simulated effective irradiance.

The nominal energy of the array at standard testing conditions (STC) following PV conversion is 11682.831 MWh. The PV array is 19.66% efficient at STC. The PV conversion bifaciality factor is 0.80. The annual virtual energy supply from MPP is 9474.405 MWh. Ohmic wiring losses make for 0.15% of the losses in this stage, while thermal loss accounts for 6.64%, module degradation loss accounts for 7.80% and modular array mismatch for 5.1%.

The inverter power plant has 9317.134 MWh of available energy per year with minor losses like inverter loss during operation is 1.66%. It feeds 9183.192 MWh amount of energy per year to the grid due to AC ohmic loss 1.15% and medium voltage transformer loss 1.07%.

The bifacial rear gain of 5.40%, when the rows are far apart the sky view factor from the rear of the panel is much higher meaning more diffuse sky radiation reaches the rear face directly and not blocked by adjacent panel rows.

The temperature loss of 6.64% is resulted from the thermal constant Uc (50 W/m^2) means PVsyst assume the modules dissipate heat more efficiently (stay cooler).

4.5. PVSYST Modeling

The Photovoltaic System (PVSYST) software was used for the FPV system's detailed design and modeling. The meteorological data is chosen from the list of databases in the PVSYST program following the entry of the case study site coordinates. The system design comprises a parallel connection of two group of sub-arrays.

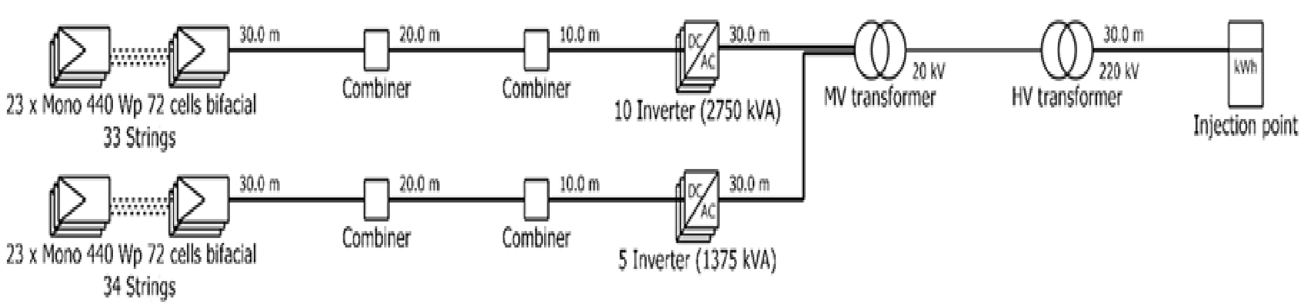

Figure 4. 8 First and Second group solar panel modeling using PVsyst software

First group contains 2 group of strings; first string contains 33 string per inverter for 10 units and second 34 per inverter for 5 units pass through DC combiner over 30m cable runs to Huawei SUN2000-330KTL inverters, whose 800 Vac output is collected and stepped up through a single 20 Kv medium voltage transform, then to a 220Kv high voltage transformer, and finally to the grid injection point. Layout of the Floating solar panel System on the GERD reservoir:

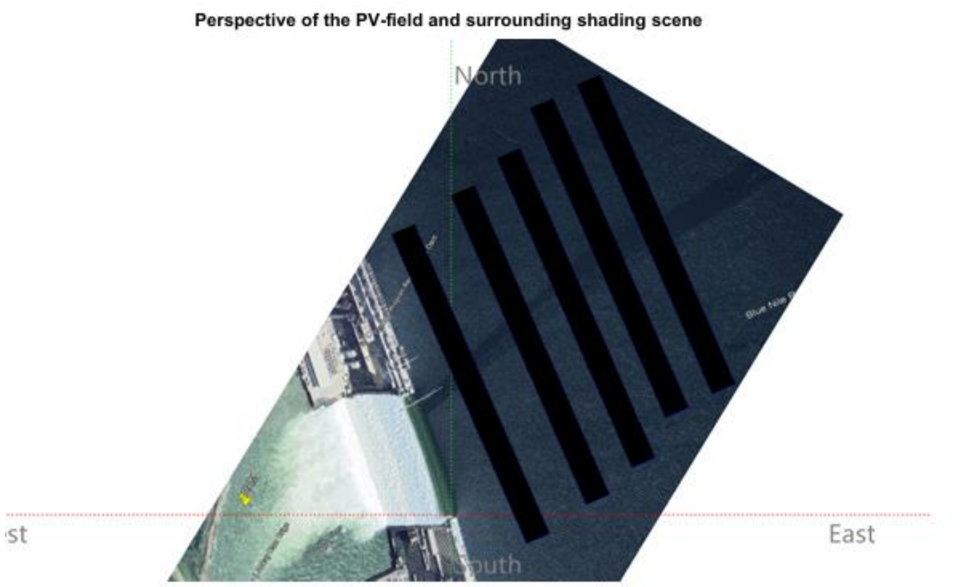

Figure 4. 9 View of the surrounding shade landscape and the PV field

4.6. Evaporation reduction

The table shown below shows the evaporation of free water surface, large foot print and small footprint on the GERD dam taken 2023 yearly data from NASA/POWER Source Native Resolution Daily Data, 01/01/2023 through 12/31/2023 in LST and Location: latitude 11.2134 longitude 35.0984. Since the area cover is 20% of 1 Km^2, x=0.2

Table 4. 3 Evaporation effect

Months	E_F (Mm ^{3}/month) losses	E_{FS} (Mm ^{3}/month) losses	E_{FL} (Mm^3/month) losses
January	8.885007986	8.050543858	7.108006389

February	11.44141653	10.57857592	9.153133227
March	14.51079589	13.80825383	11.60863672
April	13.68446144	13.00416811	10.94756915
May	11.566513	10.89270559	9.253210403
June	5.257252865	4.903958112	4.205802292
July	4.493760253	4.156031828	3.595008202
August	4.081576781	3.772903447	3.265261425
September	4.348405127	4.012544433	3.478724101
October	4.946535694	4.462009783	3.957228555
November	5.746582242	5.127707791	4.597265794
December	7.624758461	6.751472336	6.099806769
Total	96.58707	89.52088	77.26965

The annual water saved by using Small FPV is (96.58707-89.52088) mm^3= 7.066 mm^3/year

The annual water saved by using large FPV is (96.58707-77.26965) mm^3= 19.317 mm^3/year

Percentage Evaporation reduction

$$E_{FS} = \frac{E_F - E_{FS}}{E_F} = \frac{96.58707 - 89.52088}{96.58707} = \frac{7.066}{96.58707} \times 100\% = 7.32\%$$

$$E_{FL} = \frac{E_F - E_{FL}}{E_F} = \frac{96.58707 - 77.26965}{96.58707} = \frac{19.317}{96.58707} \times 100\% = 20\%$$

When compared to the open water surface situation, the monthly evaporation results show that floating photovoltaic (FPV) coverage can significantly lower reservoir water losses. The small FPV and large FPV footprint scenarios decreased evaporation to 89.521 Mm^3/year and 77.270 Mm^3/year, respectively, whereas the anticipated yearly evaporation from the open reservoir surface was 96.587 Mm^3/year. This translates to water savings of 7.066 Mm^3/year for the small FPV configuration and 19.317 Mm^3/year for the large FPV configuration, corresponding to 7.32% and 20.0% reductions in evaporation, respectively. These results show that FPV deployment on GERD can produce renewable energy and significantly reduce water usage.

Table 4. 4 Evaporation Reduction

Scenarios	Annual Evaporation (Mm³/year)	Annual Water saved (Mm³/year)	Evaporation Reduction (%)
Open water surface	96.587	0	0
Small FPV cover	89.521	7.066	7.32%
Large FPV cover	77.270	19.317	20.0 %

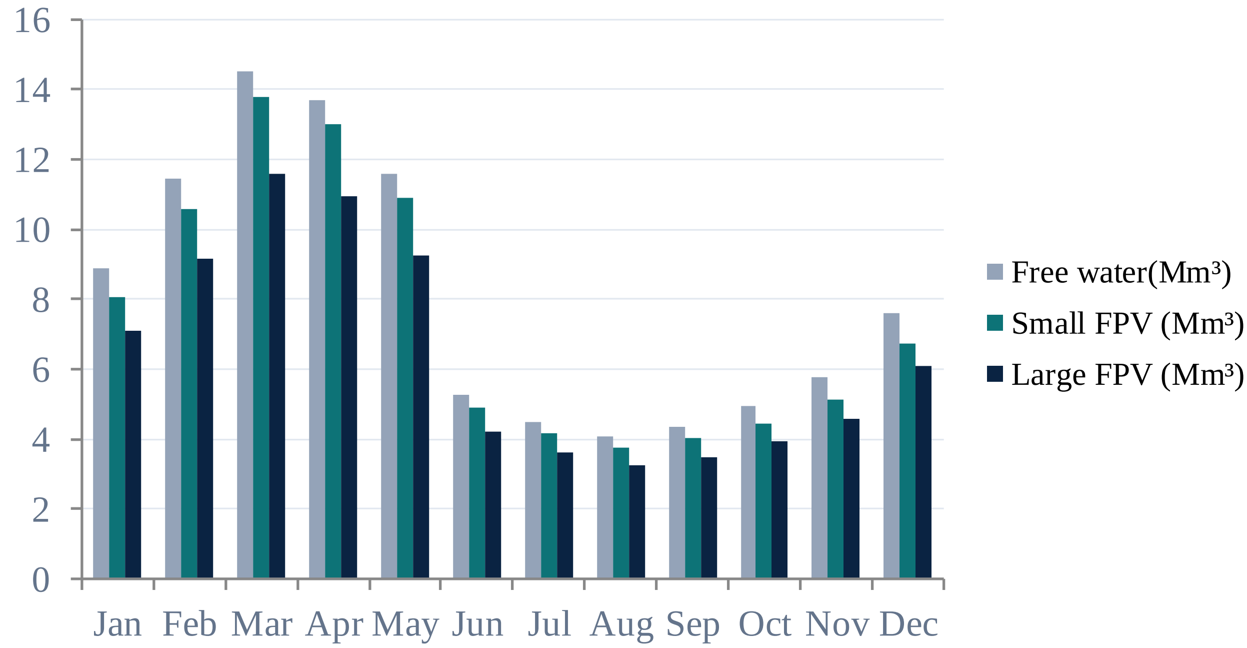

Figure 4. 10 Evaporation in mm^3 graph

4.7. Economic analysis

The key assumptions taken for the system economic analysis is:

Table 4. 5. Cost of system as entered in PVsyst

Parameters	Quantity	Unit cost (ETB)	Total (ETB)
PV modules	11,500	15,000	172,500,000
Supporter for modules	11,500	3000	34,500,000
Inverter	15	10,000	150,000
Global installation cost	11,500	3000	34500,000
Total			241,650,000

Table 4. 6. Capital expenditure

Components	Cost per Wp($)	Total Cost(5.06 MWp) in $	Total (ETB at 159)
PV module (440Wp x11500)	0.26/WP	1,315,600	209,180,400
Floating structure and pontoons	0.30/WP	1,518,000	241,362,000
Inverters(11 x Huawei)	0.1/WP	506,000	80,454,000
MV/HV transformer and switchgear	0.08/WP	404,800	64,363,200
DC/AC cabling and connectors	0.07/WP	354,200	56,317,800
Mooring/anchoring system	0.08/WP	404,800	64,363,200
Civil and marine works	0.05/WP	253,000	40,227,000
Contingency (5%)	0.051/WP	258,060	41,031,540
Total Capital Expenditure	0.991/Wp	5,014,460	797,299,140

Table 4. 7. Annual Operating and maintenance expenditure

Items	Annual cost($)/year	ETB/year
O & M labor and spare parts (1.5 % of Capital expenditure)	81,289	12,924,935
Insurance (0.5% of Capital expenditure)	27,096	4,308,312
Asset management and monitoring	10,000	1,590,000
Total annual O & M expenditure	118,385	18,823,265

Recommended realistic tariff assumption for 2026 in Grid – export (ETB 7.16/KWh or USD0.045/KWH and in Captive avoided cost diesel facilities (ETB 52.47/KWh or USD 0.33/KWh).

Pure grid export: $Year\ 1\ revenue = 9183192\ KWh \times 7.16/KWh = 65{,}751{,}654.72 ETB/year$

$$NCF = 65{,}751{,}654.72 - 18{,}823{,}265 = 46{,}928{,}389.72\ ETB/year$$

$$SP = \frac{797{,}299{,}140 \text{ ETB}}{46{,}928{,}389.72\ ETB/year} = 16.98\ years$$

Blended (10 % Captive at 52.47 ETB and 90 % grid at 7.16 ETB):

$$CR = 10\%(9183192) \times 52.47 = 48{,}184{,}208.4\ ETB$$

$$GR = 90\%(9183192) \times 7.16 = 59{,}176{,}489.24\ ETB$$

$$Total = 107{,}360{,}697.648$$

$$NCF = 107{,}360{,}697.648 - 18{,}823{,}265 = 88{,}537{,}432.64\ ETB/year$$

$$SP = \frac{797{,}299{,}140 \text{ ETB}}{88{,}537{,}432.64\ \ ETB/year} = 9.005\ years$$

High Captive (25% Captive at 52.47 ETB and 75% grid at 7.16 ETB):

$$HCR = (25\%(9183192) \times 52.47) + (75\%(9183192) \times 7.16) = 169{,}774{,}262.04ETB$$

$$NCF = 169{,}774{,}262.04 - 18{,}823{,}265 = 150{,}950{,}997.04\ ETB/year$$

$$SP = \frac{797{,}299{,}140 \text{ ETB}}{150{,}950{,}997.04\ ETB/year} = 5.28\ years$$

Where NCF is Net Cash Flow, SP is Simple Payback period, CR is Captive revenue, GR is Grid Revenue and HCR is high captive reveue.

LCOE is the minimum price per KWh at which energy must be sold to break even over the projects lifetime. Calculate the capital recovery factor (CRF) with discount rate is 8% and the period is 25 years. Where ACXP is annualized capital expenditure.

$$CRF = \frac{0.08(0.08+1)^{25}}{(1+0.08)^{25}-1} = 0.09368$$

$$ACXP\ \ = \$5{,}014{,}460\text{x } 0.09368 = \ \$469{,}754.61$$

$$LCOE = \frac{\$\ 469{,}754.61\ + \$118{,}385}{9183192\ KWh} = \frac{\$0.064}{KWh} = 10.176\ ETB/KWh$$

The levelized cost of energy is competitive with the general service grid tariff (4.01 ETB/KWh). This compares favorably with regional solar PPA benchmarks ($0.04-0.07/KWh), and Ethiopian grid electricity cost ($0.03-0.07/KWh).

4.8. Comparing the Research Results with those of other Researchers

The main hybrid finding in (EliGetieas Mandefro & Jember, 2022) the GERD has the potential to host up to 18,740 MW of FPV if 10% of its reservoir area is used, which could operate in parallel with the existing hydropower plant. To generate 1 MWp of power, 2,500 PV panels with a capacity of 400 Wp each are required. The designed system is a 1 MWp FPV system. The FPV covered area is 10,000 m² (derived from the context that 1 kWp requires 10 m²).

To generate 420 MWp of power, approximately 500,000 PV panels (285 Wp each) are required (Alhassan et al., 2023). The FPV covered area is 2.46 km² (2,460,457 m²). To generate 116 MWp, 99,996 PV modules (400 Wp each) are used. The system uses 962 inverters (40 kWac each). These are string inverters, not central inverters.

(Alhassan et al., 2023) the study models a 40 MW hydropower plant at Nam Mang 3, for the complementarity analysis. For this site, a 40 MW FSPV installed would generate a monthly average of 5.43 GWh during the dry season and 4.20 GWh during the rainy season. The proposed FPV system is 116 MWp (DC) / 100 MWac. The area required is approximately 0.224 km².

(Nguyen et al., 2023)The designed system is 47.5 MWp. The total water surface area used is 50 hectares (500,000 m²). The total area of the PV modules themselves is 279,294 m². To generate 47.5 MWp, 143,940 PV modules (72-cell, 330 Wp each) are required. The system uses 17 central inverters (2,500 kW each).

(Kimura et al., 2023) the proposed FPV system is 40 MWp. The FPV covered area is approximately 0.224 km². To generate 40 MWp, 99,996 PV modules (400 Wp each) are required. The system uses 962 inverters (40 kWac string inverters). With a 40 MWp FSPV installed, the hybrid system would generate a monthly average of 5.43 GWh during the dry season (Nov-April) and 4.20 GWh during the rainy season (May-Oct).

A comparison of the proposed FPV system with findings reported in the above indicates that the obtained results are generally consistent with those of other researchers, with only minor variations. The designed system utilizes a water surface area of 200,000 m^2 and achieves an installed capacity of 29.81 MWp using bifacial floating photovoltaic technology. In addition, the system attains a performance ratio of 73.9%, which falls within the range reported in the literature for similar FPV installations. The slight deviations observed may be attributed to differences in site-specific conditions, solar resource availability, system configuration, environmental factors, and modeling assumptions. Overall, the comparison validates the reliability and feasibility of the proposed design and demonstrates its comparable performance to existing FPV systems reported in previous studies.

CHAPTER FIVE

5. CONCLUSION AND RECOMMENDATION

5.1. Conclusion

The technical and economic feasibility analysis of 5060 KWp floating bifacial photovoltaic system installed on the Grand Ethiopian Renaissance Dam were evaluated in this study. The system comprising 11,500 monocrystalline bifacial module of 440 Wp each, configured as 500 strings of 23 modules in series and connected through 15 Huawei SUN2000-330KTL inverters, is able of generating 9,183.19 MWh of clean electricity in the first year of operation, and gradually decrease to 8,752 MWh by year 25 due to natural module degradation at a rate of 0.4% per year.

A floating solar PV system with an installed capacity of 5.06 MWp was constructed and simulated in PVsyst using a very small portion of the reservoir surface area. The suggested system attained a performance ratio of 80.18%, suggesting good operational efficiency, according to the simulation findings. The produced use full energy was determined to be 4.97 kWh/kWp/day, and system losses were comparatively low. System losses were also demonstrated to be caused by a number of problems, such as heat losses, module degradation, array mismatch losses, shading effects, and wire losses.

Despite these losses, the suggested FPV system can generate about 9,183,192 MWh of electricity per year, and using bifacial solar modules can boost energy output even more. The results determine that integrating the proposed floating photovoltaic (FPV) system with the existing hydropower plant enhances the overall energy productivity of the reservoir.

The results demonstrate that FPV arrangement can significantly mitigate reservoir evaporation losses. Compared with the open-water condition (96.587 Mm^3/year), the small FPV footprint reduced evaporation to 89.521 Mm^3/year, saving 7.066 Mm^3/year (7.32%), while the large FPV footprint reduced evaporation to 77.270 Mm^3/year, saving 19.317 Mm^3/year (20.0%). These findings indicate that larger FPV coverage provides substantially greater water-conservation benefits and can be an effective strategy for reducing evaporation from reservoirs.

The Levelized Cost of Energy calculated using Capital Recovery Factor of 0.09368 at an 8% discount rate over 25 ears, is 10.176 ETB/KWh ($ 0.064/KWh) which is competitive with regional utility-scale solar benchmarks of $0.04-0.07/KWh.

In general, the study's conclusions demonstrate that building floating solar PV systems on large reservoirs like the GERD to increase Ethiopia's capacity for renewable energy is both technically feasible and beneficial. This hybrid hydro-solar approach can support sustainable energy growth and assist the country fulfill its growing electricity needs.

5.2. Recommendation for Future Work

Since the study's findings support the viability of floating solar PV systems on the GERD reservoir, more research is advised to improve the systems' performance and deployment. First, a detailed economic and financial analysis should be conducted to evaluate the cost-effectiveness, investment requirements, and payback period of large-scale FPV installations. Future studies should also look into how floating solar systems affect aquatic ecosystems and reservoir water quality.

The literature review revealed that in addition to solar radiation, environmental factors like wind action and surrounding temperature variation affects the performance FPV. It is necessary that further studies should focus on the structural stability and durability of floating platforms under varying environmental conditions, including wind, waves, and water-level fluctuation. Determining the maximum energy output capacity of floating solar systems would also be aided by extending the investigation to a broader reservoir coverage area of the reservoir.

To further enhance system performance and grid stability, future research may investigate the integration of energy storage systems with advanced photovoltaic technologies, such as solar tracking systems and bifacial modules.

REFERENCE

Abid, M., Abid, Z., Sagin, J., Murtaza, R., Sarbassov, D., & Shabbir, M. (2019). Prospects of floating photovoltaic technology and its implementation in Central and South Asian Countries. In *International Journal of Environmental Science and Technology* (Vol. 16, Number 3, pp. 1755–1762). Center for Environmental and Energy Research and Studies. https://doi.org/10.1007/s13762-018-2080-5

Agrawal, K. K., Jha, S. K., Mittal, R. K., & Vashishtha, S. (2022). Assessment of floating solar PV (FSPV) potential and water conservation: Case study on Rajghat Dam in Uttar Pradesh, India. *Energy for Sustainable Development*, *66*, 287–295. https://doi.org/10.1016/J.ESD.2021.12.007

Alhassan, M. O., Opoku, R., Uba, F., Obeng, G. Y., Sekyere, C. K. K., & Nyanor, P. (2023). Techno-economic and environmental estimation assessment of floating solar PV power generation on Akosombo dam reservoir in Ghana. *Energy Reports*, *10*, 2740–2755. https://doi.org/10.1016/j.egyr.2023.09.073

Amer, A., Attar, H., As'ad, S., Alsaqoor, S., Colak, I., Alahmer, A., Alali, M., Borowski, G., Hmada, M., & Solyman, A. (2023). Floating Photovoltaics: Assessing the Potential, Advantages, and Challenges of Harnessing Solar Energy on Water Bodies. *Journal of Ecological Engineering*, *24*(10), 324–339. https://doi.org/10.12911/22998993/170917

Asmy, S., & Arshad, S. (n.d.). *ANALYSING, PRIORITISING AND DESIGNING OF FLOATING PHOTOVOLTAIC STRUCTURES TO BE INSTALLED IN RESERVOIRS, LAKES AND RIVERS IN SRI LANKA*.

Baloch, A. A. B., Hammat, S., Figgis, B., Alharbi, F. H., & Tabet, N. (2020). In-field characterization of key performance parameters for bifacial photovoltaic installation in a desert climate. *Renewable Energy*, *159*, 50–63. https://doi.org/10.1016/J.RENENE.2020.05.174

Benjamins, S., Williamson, B., Billing, S. L., Yuan, Z., Collu, M., Fox, C., Hobbs, L., Masden, E. A., Cottier-Cook, E. J., & Wilson, B. (2024). Potential environmental impacts of floating solar photovoltaic systems. *Renewable and Sustainable Energy Reviews*, *199*, 114463. https://doi.org/10.1016/J.RSER.2024.114463

Bernt Lamark, B., Anders Lindberg, S., Rudolf Wegelin, S., Engstedt, L., & Sweden, Z. (1998). *To be presented at 31st IMIA Meeting*. http://www.imia.com.

Bontempo Scavo, F., Tina, G. M., Gagliano, A., & Nižetić, S. (2021). An assessment study of evaporation rate models on a water basin with floating photovoltaic plants. *International Journal of Energy Research*, *45*(1), 167–188. https://doi.org/10.1002/er.5170

Cazzaniga, R., Cicu, M., Rosa-Clot, M., Rosa-Clot, P., Tina, G. M., & Ventura, C. (2018a). Floating photovoltaic plants: Performance analysis and design solutions. *Renewable and Sustainable Energy Reviews*, *81*, 1730–1741. https://doi.org/10.1016/J.RSER.2017.05.269

Cazzaniga, R., Cicu, M., Rosa-Clot, M., Rosa-Clot, P., Tina, G. M., & Ventura, C. (2018b). Floating photovoltaic plants: Performance analysis and design solutions. *Renewable and Sustainable Energy Reviews*, *81*, 1730–1741. https://doi.org/10.1016/J.RSER.2017.05.269

Cazzaniga, R., Rosa-Clot, M., Rosa-Clot, P., & Tina, G. M. (2019). Integration of PV floating with hydroelectric power plants. In *Heliyon* (Vol. 5, Number 6). Elsevier Ltd. https://doi.org/10.1016/j.heliyon.2019.e01918

Chen, Y., Ahmed, M., Tangdamrongsub, N., & Murgulet, D. (2021). Reservoir-induced land deformation: Case study from the grand ethiopian renaissance dam. *Remote Sensing*, *13*(5), 1–16. https://doi.org/10.3390/rs13050874

Chico Hermanu, B. A., Santoso, B., Suyitno, & Wicaksono, F. X. R. (2019). Design of 1 MWp floating solar photovoltaic (FSPV) power plant in Indonesia. *AIP Conference Proceedings*, *2097*. https://doi.org/10.1063/1.5098188

Conference Services Ltd, W. (2022). *Proceedings of the 21st International Ship and Offshore International Ship and Offshore, Volume II*. http://onepetro.org/snameissc/proceedings-pdf/ISSC22V2/1-ISSC22V2/D011S001R007/3099100/sname-issc-2022-committee-v-6.pdf/1

Degefu, D. M., He, W., & Zhao, J. H. (2015). Hydropower for sustainable water and energy development in Ethiopia. *Sustainable Water Resources Management*, *1*(4), 305–314. https://doi.org/10.1007/s40899-015-0029-0

Design and analysis for a feasibility study of a floating solar PV power system for Metolong Dam. (2022).

Design and Implementation of a Floating PV Model to Analyse. (n.d.).

Di Grazia, S., & Tina, G. M. (2024). Optimal site selection for floating photovoltaic systems based on Geographic Information Systems (GIS) and Multi-Criteria Decision Analysis (MCDA): a case study. *International Journal of Sustainable Energy*, *43*(1). https://doi.org/10.1080/14786451.2023.2167999

Do Sacramento, E. M., Carvalho, P. C. M., De Araújo, J. C., Riffel, D. B., Da Cruz Corrêa, R. M., & Neto, J. S. P. (2015). Scenarios for use of floating photovoltaic plants in Brazilian reservoirs. *IET Renewable Power Generation*, *9*(8), 1019–1024. https://doi.org/10.1049/iet-rpg.2015.0120

Du, S., Liang, C., Sun, H., Wang, K., Wang, J., Li, H., Xue, J., Chen, F., Tuo, Y., Disse, M., & Zhang, W. (2024). Evaluating the potential benefits of float solar photovoltaics through the water footprint recovery period. *Journal of Cleaner Production*, *446*, 141399. https://doi.org/10.1016/J.JCLEPRO.2024.141399

EliGetieas Mandefro, & Jember, Y. B. (2022). Potential Assessment and Performance Evaluation of a Floating Solar Photovoltaic on the Great Ethiopian Renaissance Dam. *International Journal of Photoenergy*, *2022*. https://doi.org/10.1155/2022/6964984

Elminshawy, N. A. S., Mohamed, A. M. I., Osama, A., Amin, I., Bassam, A. M., & Oterkus, E. (2022). Performance and potential of a novel floating photovoltaic system in Egyptian winter climate on calm water surface. *International Journal of Hydrogen Energy*, *47*(25), 12798–12814. https://doi.org/10.1016/J.IJHYDENE.2022.02.034

Exley, G., Armstrong, A., Page, T., & Jones, I. D. (2021). Floating photovoltaics could mitigate climate change impacts on water body temperature and stratification. *Solar Energy*, *219*, 24–33. https://doi.org/10.1016/J.SOLENER.2021.01.076

Exley, G., Page, T., Thackeray, S. J., Folkard, A. M., Couture, R. M., Hernandez, R. R., Cagle, A. E., Salk, K. R., Clous, L., Whittaker, P., Chipps, M., & Armstrong, A. (2022). Floating solar panels on reservoirs impact phytoplankton populations: A modelling experiment. *Journal of Environmental Management*, *324*, 116410. https://doi.org/10.1016/J.JENVMAN.2022.116410

Farfan, J., & Breyer, C. (2018). Combining Floating Solar Photovoltaic Power Plants and Hydropower Reservoirs: A Virtual Battery of Great Global Potential. *Energy Procedia*, *155*, 403–411. https://doi.org/10.1016/J.EGYPRO.2018.11.038

Farrar, L. W., Bahaj, A. B. S., James, P., Anwar, A., & Amdar, N. (2022). Floating solar PV to reduce water evaporation in water stressed regions and powering water pumping: Case study Jordan. *Energy Conversion and Management*, *260*. https://doi.org/10.1016/j.enconman.2022.115598

Feng, Y., Liu, Q., Qu, Y., & Liang, S. (2016). Estimation of the Ocean Water Albedo From Remote Sensing and Meteorological Reanalysis Data. *IEEE Transactions on Geoscience and Remote Sensing*, *54*(2), 850–868. https://doi.org/10.1109/TGRS.2015.2468054

Floating photovoltaics may reduce the risk of hydro-dominated energy development in Africa, 12 April 2024. (n.d.).

floating Solar panel A solution for climate change and energy efficency. (n.d.).

Gadzanku, S., Mirletz, H., Lee, N., Daw, J., & Warren, A. (2021). Benefits and critical knowledge gaps in determining the role of floating photovoltaics in the energy-water-food nexus. *Sustainability (Switzerland)*, *13*(8). https://doi.org/10.3390/su13084317

Ghosh, A. (2022). Fenestration integrated BIPV (FIPV): A review. *Solar Energy*, *237*, 213–230. https://doi.org/10.1016/J.SOLENER.2022.04.013

Ghosh, A. (2023). A comprehensive review of water based PV: Flotavoltaics, under water, offshore & canal top. *Ocean Engineering*, *281*, 115044. https://doi.org/10.1016/J.OCEANENG.2023.115044

Gonzalez Sanchez, R., Kougias, I., Moner-Girona, M., Fahl, F., & Jäger-Waldau, A. (2021). Assessment of floating solar photovoltaics potential in existing hydropower reservoirs in Africa. *Renewable Energy*, *169*, 687–699. https://doi.org/10.1016/J.RENENE.2021.01.041

Gorjian, S., Sharon, H., Ebadi, H., Kant, K., Scavo, F. B., & Tina, G. M. (2021). Recent technical advancements, economics and environmental impacts of floating photovoltaic solar energy conversion systems. *Journal of Cleaner Production*, *278*, 124285. https://doi.org/10.1016/J.JCLEPRO.2020.124285

Guerrero-Lemus, R., Vega, R., Kim, T., Kimm, A., & Shephard, L. E. (2016). Bifacial solar photovoltaics – A technology review. *Renewable and Sustainable Energy Reviews*, *60*, 1533–1549. https://doi.org/10.1016/J.RSER.2016.03.041

Gunfaus, M. T., & Waisman, H. (2021). Assessing the adequacy of the global response to the Paris Agreement: Toward a full appraisal of climate ambition and action. *Earth System Governance*, *8*. https://doi.org/10.1016/j.esg.2021.100102

Gu, W., Ma, T., Ahmed, S., Zhang, Y., & Peng, J. (2020a). A comprehensive review and outlook of bifacial photovoltaic (bPV) technology. *Energy Conversion and Management*, *223*. https://doi.org/10.1016/j.enconman.2020.113283

Gu, W., Ma, T., Ahmed, S., Zhang, Y., & Peng, J. (2020b). A comprehensive review and outlook of bifacial photovoltaic (bPV) technology. *Energy Conversion and Management*, *223*, 113283. https://doi.org/10.1016/J.ENCONMAN.2020.113283

Haas, J., Khalighi, J., de la Fuente, A., Gerbersdorf, S. U., Nowak, W., & Chen, P. J. (2020). Floating photovoltaic plants: Ecological impacts versus hydropower operation flexibility. *Energy Conversion and Management*, *206*, 112414. https://doi.org/10.1016/J.ENCONMAN.2019.112414

Hafeez, H., Kashif Janjua, A., Nisar, H., Shakir, S., Shahzad, N., & Waqas, A. (2022). Techno-economic perspective of a floating solar PV deployment over urban lakes: A case study of

NUST lake Islamabad. *Solar Energy*, *231*, 355–364. https://doi.org/10.1016/J.SOLENER.2021.11.071

Hijazin, M. I. (1998). The diffuse fraction of hourly solar radiation for Amman/Jordan. *Renewable Energy*, *13*(2), 249–253. https://doi.org/10.1016/S0960-1481(97)00082-7

Ineichen, P., Guisan, O., & Perez, R. (1990). Ground-reflected radiation and albedo. *Solar Energy*, *44*(4), 207–214. https://doi.org/10.1016/0038-092X(90)90149-7

IREC2015 International Renewable Energy Congress : the Sixth International Renewable Energy Congress : 2015 6th International Renewable Energy Congress (IREC), March 24-26, 2015, Sousse, Tunisia. (2015). IEEE.

Irshad, A. S., Ahmad Ludin, G., Ludin, S., Elkholy, M. H., Elias, S., & Senjyu, T. (2024). Integration and performance analysis of optimal large-scale hybrid PV and pump hydro storage system based upon floating PV for practical application. *Energy Conversion and Management: X*, *22*. https://doi.org/10.1016/j.ecmx.2024.100599

Jiang, Z., Dai, J., Saettone, S., Tørå, G., He, Z., Bashir, M., & Souto-Iglesias, A. (2023). Design and model test of a soft-connected lattice-structured floating solar photovoltaic concept for harsh offshore conditions. *Marine Structures*, *90*, 103426. https://doi.org/10.1016/J.MARSTRUC.2023.103426

Kaplanis, S., Kaplani, E., & Kaldellis, J. K. (2023). PV Temperature Prediction Incorporating the Effect of Humidity and Cooling Due to Seawater Flow and Evaporation on Modules Simulating Floating PV Conditions. *Energies*, *16*(12). https://doi.org/10.3390/en16124756

Kimura, S., Sudo, K., Ryota, A., & Komatsubara, K. K. (2023). *Effectiveness of the Hybrid System Combining Hydropower and Floating Solar in the Lao PDR*.

Koondhar, M. A., Albasha, L., Mahariq, I., Graba, B. B., & Touti, E. (2024). Reviewing floating photovoltaic (FPV) technology for solar energy generation. *Energy Strategy Reviews*, *54*, 101449. https://doi.org/10.1016/J.ESR.2024.101449

Kougias, I., Bódis, K., Jäger-Waldau, A., Monforti-Ferrario, F., & Szabõ, S. (2016). Exploiting existing dams for solar PV system installations. *Progress in Photovoltaics: Research and Applications*, *24*(2), 229–239. https://doi.org/10.1002/pip.2640

Kumar, M., Mohammed Niyaz, H., & Gupta, R. (2021). Challenges and opportunities towards the development of floating photovoltaic systems. *Solar Energy Materials and Solar Cells*, *233*, 111408. https://doi.org/10.1016/J.SOLMAT.2021.111408

Lee, N., Grunwald, U., Rosenlieb, E., Mirletz, H., Aznar, A., Spencer, R., & Cox, S. (2020). Hybrid floating solar photovoltaics-hydropower systems: Benefits and global assessment of technical potential. *Renewable Energy*, *162*, 1415–1427. https://doi.org/10.1016/J.RENENE.2020.08.080

Li, M., Luo, H., Zhou, S., Senthil Kumar, G. M., Guo, X., Law, T. C., & Cao, S. (2022). State-of-the-art review of the flexibility and feasibility of emerging offshore and coastal ocean energy technologies in East and Southeast Asia. *Renewable and Sustainable Energy Reviews*, *162*, 112404. https://doi.org/10.1016/J.RSER.2022.112404

Liu, H., Krishna, V., Lun Leung, J., Reindl, T., & Zhao, L. (2018). Field experience and performance analysis of floating PV technologies in the tropics. *Progress in Photovoltaics: Research and Applications*, *26*(12), 957–967. https://doi.org/10.1002/pip.3039

Luo, W., Isukapalli, S. N., Vinayagam, L., Ting, S. A., Pravettoni, M., Reindl, T., & Kumar, A. (2021). Performance loss rates of floating photovoltaic installations in the tropics. *Solar Energy*, *219*, 58–64. https://doi.org/10.1016/J.SOLENER.2020.12.019

Ma, C., Wu, R., Liu, Z., & Li, X. (2024). Performance assessment of different photovoltaic module technologies in floating photovoltaic power plants under waters environment. *Renewable Energy*, *222*, 119890. https://doi.org/10.1016/J.RENENE.2023.119890

Mahmood, S., Deilami, S., & Taghizadeh, S. (2021). Floating Solar PV and Hydropower in Australia: Feasibility, Future Investigations and Challenges. *Proceedings of 2021 31st Australasian Universities Power Engineering Conference, AUPEC 2021*. https://doi.org/10.1109/AUPEC52110.2021.9597714

MARCO ROSA-CLOT. (2018). Front Matter. In *Submerged and Floating Photovoltaic Systems* (pp. i–iii). Elsevier. https://doi.org/10.1016/b978-0-12-812149-8.09987-7

Masaki Umejim 2021. (n.d.).

mathematical simulation. (n.d.).

Matheus, M. N., & Musti, K. S. S. (2023). *Design and Simulation of a Floating Solar Power Plant for Goreagab Dam, Namibia* (pp. 1–26). https://doi.org/10.4018/978-1-6684-4118-3.ch001

Mayville, P., Patil, N. V., & Pearce, J. M. (2020). Distributed manufacturing of after market flexible floating photovoltaic modules. *Sustainable Energy Technologies and Assessments*, *42*, 100830. https://doi.org/10.1016/J.SETA.2020.100830

Micheli, L. (2022). The temperature of floating photovoltaics: Case studies, models and recent findings. *Solar Energy*, *242*, 234–245. https://doi.org/10.1016/J.SOLENER.2022.06.039

Moraes, C. A., Valadão, G. F., Renato, N. S., Botelho, D. F., Oliveira, A. C. L. de, Aleman, C. C., & Cunha, F. F. (2022). Floating photovoltaic plants as an electricity supply option in the Tocantins-

Araguaia basin. *Renewable Energy*, *193*, 264–277. https://doi.org/10.1016/J.RENENE.2022.04.142

Nasir, J., Javed, A., Ali, M., Ullah, K., & Kazmi, S. A. A. (2023). Sustainable and cost-effective hybrid energy solution for arid regions: Floating solar photovoltaic with integrated pumped storage and conventional hydropower. *Journal of Energy Storage*, *74*, 109417. https://doi.org/10.1016/J.EST.2023.109417

Nguyen, N. H., Le, B. C., Nguyen, L. N., & Bui, T. T. (2023). Technical Analysis of the Large Capacity Grid-Connected Floating Photovoltaic System on the Hydropower Reservoir. *Energies*, *16*(9). https://doi.org/10.3390/en16093780

Niccolai, A., Grimaccia, F., Lorenzo, G. Di, Araneo, R., Ughi, F., & Polenghi, M. (2024). A Review of Floating PV Systems With a Techno-Economic Analysis. *IEEE Journal of Photovoltaics*, *14*(1), 23–34. https://doi.org/10.1109/JPHOTOV.2023.3319601

Oliveira-Pinto, S., & Stokkermans, J. (2020). Assessment of the potential of different floating solar technologies – Overview and analysis of different case studies. *Energy Conversion and Management*, *211*. https://doi.org/10.1016/j.enconman.2020.112747

Osama, A., Tina, G. M., Mannino, G., Cucuzza, A. V., & Bizzarri, F. (2017). *Date of publication xxxx 00, 0000, date of current version xxxx 00, 0000. Experimental and Numerical Performance Assessment of East-West Bifacial Photovoltaic Floating System in Freshwater Basins*. *XX*. https://doi.org/10.1109/ACCESS.2022.Doi

Pakyala, H. B. S. (2021). Floating Solar Potential Assessment. *Asia-Pacific Power and Energy Engineering Conference, APPEEC*, *2021-November*. https://doi.org/10.1109/APPEEC50844.2021.9687733

Patil, A., Mamatha, G., Kulkarni, P. S., & Verma, A. (2022). Analysis of Hybrid Floating Photovoltaic and Hydro-Power plant with HOMER Pro Software. *10th IEEE International Conference on Power Electronics, Drives and Energy Systems, PEDES 2022*. https://doi.org/10.1109/PEDES56012.2022.10080502

Perera, H. D. M. R. (2020). Designing of 3MW Floating Photovoltaic Power System and its Benefits over Other PV Technologies. *International Journal of Advances in Scientific Research and Engineering*, *06*(04), 37–48. https://doi.org/10.31695/ijasre.2020.33782

Qi, L., Jiang, M., Lv, Y., Zhang, Z., & Yan, J. (2021). Techno-economic assessment of photovoltaic power generation mounted on cooling towers. *Energy Conversion and Management*, *235*. https://doi.org/10.1016/j.enconman.2021.113907

Quek, A., Ee, A., Ng, A., & Wah, T. Y. (2018). Challenges in Environmental Sustainability of renewable energy options in Singapore. *Energy Policy*, *122*, 388–394. https://doi.org/10.1016/J.ENPOL.2018.07.055

Raina, G., & Sinha, S. (2023). Experimental investigations of front and rear side soiling on bifacial PV module under different installations and environmental conditions. *Energy for Sustainable Development*, *72*, 301–313. https://doi.org/10.1016/J.ESD.2023.01.001

Rodríguez-Gallegos, C. D., Bieri, M., Gandhi, O., Singh, J. P., Reindl, T., & Panda, S. K. (2018). Mono-facial vs bifacial Si-based PV modules: Which one is more cost-effective? *Solar Energy*, *176*, 412–438. https://doi.org/10.1016/J.SOLENER.2018.10.012

Rosa-Clot, M., Tina, G. M., & Nizetic, S. (2017). Floating photovoltaic plants and wastewater basins: an Australian project. *Energy Procedia*, *134*, 664–674. https://doi.org/10.1016/J.EGYPRO.2017.09.585

Sahu, A., Yadav, N., & Sudhakar, K. (2016). Floating photovoltaic power plant: A review. *Renewable and Sustainable Energy Reviews*, *66*, 815–824. https://doi.org/10.1016/J.RSER.2016.08.051

Samaan, M. M. (2019). The Post-2011 Round: The New Chapter of the Grand Ethiopian Renaissance Dam and the Shadow of the Future. In *The Nile Development Game* (pp. 179–229). Springer International Publishing. https://doi.org/10.1007/978-3-030-02665-3_6

Shi, W., Yan, C., Ren, Z., Yuan, Z., Liu, Y., Zheng, S., Li, X., & Han, X. (2023). Review on the development of marine floating photovoltaic systems. *Ocean Engineering*, *286*, 115560. https://doi.org/10.1016/J.OCEANENG.2023.115560

Shoukry, I., Libal, J., Kopecek, R., Wefringhaus, E., & Werner, J. (2016). Modelling of Bifacial Gain for Stand-alone and in-field Installed Bifacial PV Modules. *Energy Procedia*, *92*, 600–608. https://doi.org/10.1016/J.EGYPRO.2016.07.025

Singh, Y., Singh, B., & Mishra, S. (2020, December 16). A High-Performance Solar PV Array-Wind and Battery Integrated Microgrid for Rural Electrification. *9th IEEE International Conference on Power Electronics, Drives and Energy Systems, PEDES 2020*. https://doi.org/10.1109/PEDES49360.2020.9379877

Solomin, E., Sirotkin, E., Cuce, E., Selvanathan, S. P., & Kumarasamy, S. (2021). Hybrid floating solar plant designs: A review. In *Energies* (Vol. 14, Number 10). MDPI AG. https://doi.org/10.3390/en14102751

Stiubiener, U., Carneiro da Silva, T., Trigoso, F. B. M., Benedito, R. da S., & Teixeira, J. C. (2020). PV power generation on hydro dam's reservoirs in Brazil: A way to improve operational flexibility. *Renewable Energy*, *150*, 765–776. https://doi.org/10.1016/J.RENENE.2020.01.003

structural FPV. (n.d.).

Sutanto, B., Indartono, Y. S., Wijayanta, A. T., & Iacovides, H. (2022). Enhancing the performance of floating photovoltaic system by using thermosiphon cooling method: Numerical and experimental analyses. *International Journal of Thermal Sciences*, *180*, 107727. https://doi.org/10.1016/J.IJTHERMALSCI.2022.107727

Taye, B. Z., Nebey, A. H., & Workineh, T. G. (2020). Design of floating solar PV system for typical household on Debre Mariam Island. *Cogent Engineering*, *7*(1). https://doi.org/10.1080/23311916.2020.1829275

Temiz, M., & Dincer, I. (2022). Design and analysis of a floating photovoltaic based energy system with underground energy storage options for remote communities. *Journal of Energy Storage*, *55*, 105733. https://doi.org/10.1016/J.EST.2022.105733

The 6 types of solr panels. (n.d.).

The Advantages and Disadvantages of Floating Solar MIBTE ENERGY 2024. (n.d.).

Tina, G. M., Bontempo Scavo, F., Merlo, L., & Bizzarri, F. (2021). Comparative analysis of mono-facial and bifacial photovoltaic modules for floating power plants. *Applied Energy*, *281*, 116084. https://doi.org/10.1016/J.APENERGY.2020.116084

Trapani, K., & Redõn Santafé, M. (2015). A review of floating photovoltaic installations: 2007-2013. In *Progress in Photovoltaics: Research and Applications* (Vol. 23, Number 4, pp. 524–532). John Wiley and Sons Ltd. https://doi.org/10.1002/pip.2466

Valiantzas, J. D. (2006). Simplified versions for the Penman evaporation equation using routine weather data. *Journal of Hydrology*, *331*(3–4), 690–702. https://doi.org/10.1016/j.jhydrol.2006.06.012

Velu Kaliyannan, G., Gunasekaran, R., Sivaraj, S., Jaganathan, S., & Rathanasamy, R. (2021). *4 Thin-Film Solar Cells*.

Wijewardane, S., & Kazmerski, L. L. (2023). Inventions, innovations, and new technologies: Flexible and lightweight thin-film solar PV based on CIGS, CdTe, and A-Si:H. *Solar Compass*, *7*, 100053. https://doi.org/10.1016/J.SOLCOM.2023.100053

Yousuf, E. H., Khokhar, M. Q., Zahid, M. A., & Kim, J. (n.d.). *A Review on Floating Photovoltaic Technology (FPVT)*. https://doi.org/10.21218/CPR.2020.8.3.067

Yusufoglu, U. A., Pletzer, T. M., Koduvelikulathu, L. J., Comparotto, C., Kopecek, R., & Kurz, H. (2015). Analysis of the annual performance of bifacial modules and optimization methods. *IEEE Journal of Photovoltaics*, *5*(1), 320–328. https://doi.org/10.1109/JPHOTOV.2014.2364406